

ABSTRACT

DINOVA, VINCENT ANTHONY. Automated Spectrum Stripping of Photon Spectra.
(Under the direction of Robin Pierce Gardner.)

Spectrum Stripping is a proposed method for replacing linear least squares for solving complex photon spectra. There is an inherent flaw in the linear least squares method for problems in which one or more of the libraries is unknown. In these instances, using linear least squares will cause an overshoot of the data to minimize the differences between the original and fitted spectrum. By stripping all of the known libraries in order of highest to lowest energy, it is possible to determine a better fit for the unknown spectrum.

Monte Carlo simulations were generated using the Center for Engineering Applications of Radioisotopes (CEAR) computer cluster in order to provide an experimental data set. The method of Spectrum Stripping was then presented and compared to linear least squares.

It was discovered that by performing Spectrum Stripping, a more accurate solution to the problem was found. Although an increase in the overall error was observed, the relative error was much improved leading to the conclusion that Spectrum Stripping is a viable replacement for solving complex photon spectra.

Automated Spectrum Stripping of Photon Spectra

by
Vincent Anthony DiNova

A thesis submitted to the Graduate Faculty of
North Carolina State University
in partial fulfillment of the
requirements for the Degree of
Master of Science

Nuclear Engineering
Raleigh, North Carolina

2011

APPROVED BY:

Dr. Gross

Dr. Bourham

Dr. Gardner
Chair of Advisory Committee

DEDICATION

For all the people who have given me their hearts, their minds, and their time,

For all of my teachers and others who have provoked a thought,

For the innovators, scientists, mathematicians, and engineers who have brought us here,

For my family, friends, and for those who could be considered both,

For all the people who have sacrificed their lives for our country,

I dedicate this to you, for without your deeds, this work would not have been possible

BIOGRAPHY

Vincent Anthony DiNova, Jr. was born in Orlando, FL on the 8th of July, 1986 to Kay Lynn DiNova and Vincent Anthony DiNova, Sr. Being born into a military family, his primary education was spent scattered all over the world. In 2001, his family moved to Apex, North Carolina, where he graduated from Apex High School in 2004.

After excelling in both math and science, Vincent decided to enroll at North Carolina State University. In 2009, he completed his Bachelor of Science degree in Nuclear Engineering. Upon completion, Vincent took the opportunity to continue his education under the direction of Dr. Gardner. He is currently working towards completing his Master of Science degree in Nuclear Engineering.

ACKNOWLEDGEMENTS

I would like to thank my family, whose support has always driven me to succeed. I would also like to thank all of my friends who have made life more enjoyable.

I would also like to thank all of those who have helped me in my research. A special thanks to all of the members of CEAR, who have contributed in many different areas.

Finally, I would like to thank Dr. Gardner for taking me as one of his graduate students and for all of the mentoring that he has given me along the way.

TABLE OF CONTENTS

| | |
|--|------|
| LIST OF TABLES | vii |
| LIST OF FIGURES | viii |
| Chapter 1 | 1 |
| Introduction to Spectrum Stripping | 1 |
| 1.1 Motivation..... | 1 |
| 1.2 Background..... | 1 |
| 1.3 Alternative Uses..... | 8 |
| 1.4 Analysis Involved | 9 |
| Chapter 2..... | 10 |
| New Spectrum Stripping Analysis..... | 10 |
| 2.1 Reasoning for Method..... | 10 |
| 2.2 Monte Carlo Simulations | 10 |
| 2.3 Computing Power | 11 |
| 2.4 Methods of Analysis | 12 |
| Chapter 3..... | 15 |
| Masking..... | 15 |
| 3.1 Introduction to Masking..... | 16 |
| 3.2 Analysis for Problem | 17 |
| 3.3 Results..... | 20 |
| Chapter 4..... | 32 |
| Phase Samples..... | 32 |
| 4.1 Introduction to CEARCPG | 33 |
| 4.2 Analysis..... | 36 |
| 4.2 Results..... | 37 |
| Chapter 5..... | 44 |
| Discussion..... | 44 |
| Chapter 6..... | 46 |
| Future Work..... | 46 |
| Chapter 7..... | 48 |
| Conclusions..... | 48 |
| REFERENCES | 49 |
| APPENDIX..... | 50 |
| APPENDIX A: U-235 MCNP INPUT DECK..... | 51 |

| | |
|---|----|
| APPENDIX B: CO-60 MCNP INPUT DECK..... | 53 |
| APPENDIX C: CS-137 MCNP INPUT DECK..... | 55 |

LIST OF TABLES

| | |
|---|----|
| TABLE 1: LINEAR COMBINATION OF RADIOISOTOPES FOR LOW U-235 CASE | 20 |
| TABLE 2: COMPARISON OF RESULTS..... | 25 |
| TABLE 3: LINEAR COEFFICIENTS FOR HIGH U-235 CASE..... | 28 |
| TABLE 4: COMPARISON BETWEEN EXPERIMENT AND CALCULATED VALUES | 31 |
| TABLE 5: LINEAR CORRELATION COEFFICIENTS FOR PHASE LIBRARIES | 37 |
| TABLE 6: COMPARISON BETWEEN CALCULATED AND KNOWN AMOUNTS | 43 |

LIST OF FIGURES

| | |
|---|----|
| FIGURE 1: RADIOISOTOPE CONTRIBUTION IN SALMON EXPERIMENT | 3 |
| FIGURE 2: DETECTOR RESPONSE..... | 7 |
| FIGURE 3: RELAXATION PEAKS IN AHMAD ET AL EXPERIMENT | 8 |
| FIGURE 4: CEAR COMPUTER CLUSTER..... | 12 |
| FIGURE 5: PICTURE OF AN ADVANCED SPECTROSCOPIC PORTAL | 16 |
| FIGURE 6: CS-137 OUTPUT FROM MCNP ORIGINAL DATA AND SPREAD DATA | 17 |
| FIGURE 7: CO-60 OUTPUT FROM MCNP ORIGINAL DATA AND SPREAD DATA | 18 |
| FIGURE 8: U-235 OUTPUT FROM MCNP ORIGINAL DATA AND SPREAD DATA | 19 |
| FIGURE 9: LIBRARY CONTRIBUTION TO THE ENTIRE SPECTRUM | 21 |
| FIGURE 10: EXPERIMENTAL SPECTRUM FOR LIMITED U-235 CASE..... | 22 |
| FIGURE 11: EXPERIMENTAL SPECTRUM AND FIT..... | 23 |
| FIGURE 12: RESIDUALS FOR FIT | 24 |
| FIGURE 13: BEST FIT FOR RESIDUAL | 25 |
| FIGURE 14: FIT USING LINEAR LEAST SQUARES | 26 |
| FIGURE 15: RESIDUALS USING LINEAR LEAST SQUARES METHOD..... | 27 |
| FIGURE 16: EXPERIMENTAL SPECTRUM FOR HIGH U-235 CASE | 28 |
| FIGURE 17: ORIGINAL DATA AND FIT FOR HIGH U-235 CASE..... | 29 |
| FIGURE 18: RESIDUAL FOR HIGH U-235 CASE..... | 30 |
| FIGURE 19: BEST FIT FOR THE RESIDUAL CALCULATION..... | 31 |
| FIGURE 20: VISUAL OF PROMPT GAMMA NEUTRON ACTIVATION ANALYSIS | 33 |
| FIGURE 21: CEARCPG OUTPUT FOR SALT LIBRARY | 34 |
| FIGURE 22: CEARCPG OUTPUT FOR WATER LIBRARY | 35 |
| FIGURE 23: CEARCPG OUTPUT FOR AIR LIBRARY..... | 36 |
| FIGURE 24: LIBRARY CONTRIBUTION TO EXPERIMENTAL SPECTRUM..... | 37 |
| FIGURE 25: EXPERIMENTAL SPECTRUM..... | 38 |
| FIGURE 26: FITTED DATA FOR AIR LIBRARY | 39 |
| FIGURE 27: RESIDUAL AFTER REMOVING AIR LIBRARY..... | 40 |
| FIGURE 28: FITTED DATA FOR SALT LIBRARY TO RESIDUAL..... | 41 |
| FIGURE 29: RESIDUAL AFTER REMOVING SALT LIBRARY..... | 42 |
| FIGURE 30: FITTED DATA FOR WATER LIBRARY TO STRIPPED SPECTRUM..... | 43 |

Chapter 1

Introduction to Spectrum Stripping

1.1 Motivation

Since the beginning of mathematics and science, there has been a need to express and solve problems. As history has shown, the problems have become more and more complex over time; therefore, the methods for solving problems have grown in number, variety and complexion. The method for solving problems by the use of Spectrum Stripping was first introduced in the early 1960's. Now that computer technology can create fast, accurate simulations, Spectrum Stripping should be explored as a method for solving complicated problems.

1.2 Background

Spectrum Stripping is a method of finding the contribution of a single radioisotope from a larger spectrum consisting of multiple radioisotopes, which is performed by first locating the peak of highest energy. The pulse-height detector response corresponding to this gamma-ray energy is then subtracted from the entire spectrum. The next step is to identify the next highest energy. The pulse-height detector response is then subtracted from the remaining spectrum and is repeated until there is a negligible residual remaining. The final

output will be a linear combination of each radioisotope that will make up the entire spectrum.

The first uses of Spectrum Stripping were called Graphical Analysis by Subtraction in the nuclear field due to the way the process was performed. This process is demonstrated in “Analysis of Gamma-Ray Scintillation Spectra by the Method of Least Squares” (Salmon, 1961). In Salmon’s experiment, a series of six standard sources were counted on a spectrometer for an effective period of ten minutes each. These sources were also counted in mixtures of two, three, four, and six to give a simulation of mixtures. Finally, the method of successive subtraction (or Spectrum Stripping) was used to analyze the data. Figure 1 demonstrates how this method is used.

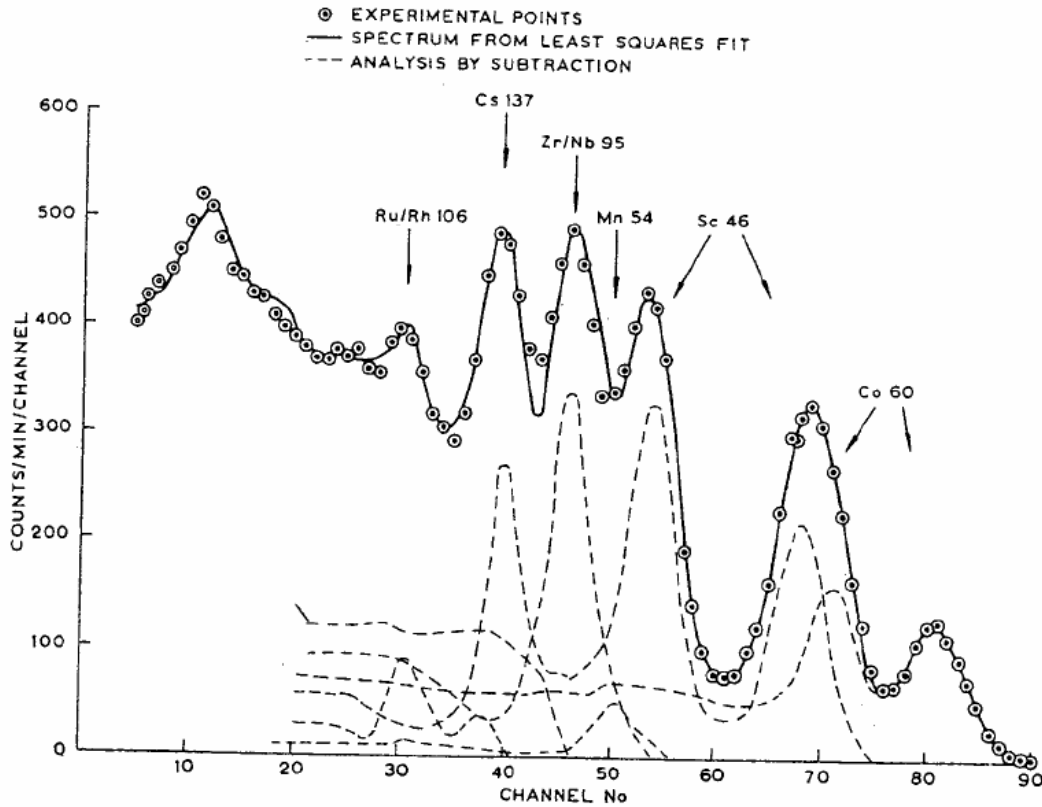


Figure 1: Radioisotope Contribution in Salmon Experiment

In this case, Co-60 is the highest energy radioisotope. The amount of Co-60 subtracted from the entire spectrum is found using graphical methods. After subtracting this from the entire spectrum, Sc-46 is the next highest energy radioisotope. The process is continued until the contribution of each radioisotope is known. Without Spectrum Stripping, it would appear that there is a large amount of Ru/Rn-106. After performing Spectrum Stripping, it is found that the contribution of this radioisotope is smaller than expected.

The results were then compared to a linear least squares fitting. It was shown that not only was the linear least squares more accurate, but the error was lower in each case.

In the early stages of using the Graphical Analysis by Subtraction method, it was discovered that not only is the analysis subjective on the user, but also takes a significant amount of time (Heath, 1966). Heath also showed that the user must have a fair amount of knowledge about energy vs. pulse-height response of the spectrometer.

Gamma-rays interact with matter to deposit their energy into a Scintillator through three different mechanisms. The first process is Photoelectric Absorption, in which the energy of a gamma-ray is completely absorbed by the atom. This excites the atom. In order to de-excite, the energy is transferred to one of the inner electrons, which is then ejected. This is known as the photoelectron. With a void in this electron shell, an outer electron then falls into this place, giving off a low energy x-ray, which generally is re-absorbed. The energy transferred to the photoelectron is equal to the energy of the photon minus the binding energy needed to remove the electron from its current bound state. Since the binding energy of electrons is small in comparison to photon energies in an order of magnitude of MeV, all of the energy must be transferred to the photoelectron. This photoelectron interacts with the Scintillator, which produces multiple ionizations, and eventually will deposit all of its energy within the detector. This interaction occurs more with an increase in atomic number, but occurs less when the photon energy is increased.

The next gamma-ray interaction is between a photon and one of the outermost electrons of an atom. Since these electrons are further from the nucleus, they are more loosely bound because the electro-static force decreases as the distance from the nucleus is

increased. Only some of the energy is given to these electrons, and the rest is kept by the scattered photon.

The final gamma-ray interaction is pair production, which is where γ -ray goes near an atom and becomes an electron-positron pair. All three of these create ionizing radiation, which can be detected by using a Scintillator.

There are many different materials that can be used for a Scintillator. These can be solids, liquids, or gases and in inorganic or organic materials. Since Scintillators need to be transparent, crystals are commonly used. Some inorganic crystals include NaI, CsI, and CsF, all of which are doped with an activator. The energy levels for the electrons in the crystal blur into two different energy levels, valence and conduction bands which are separated by a band gap. There are no natural energy states in this gap so it is the forbidden region. The use of an activator can be beneficial, because it provides energy levels in this gap. The importance of this is that when an electron is excited from the valence band to the conduction band, it leaves an opening in the valence band. To de-excite, the material must recombine with the opening, which will give off a photon with energy. Without a bridge between the conduction and valence bands, the energy of this photon will be the same as the gap, leaving a high probability of being re-absorbed by another atom, because the energy is the same as needed to excite an electron into the conduction band. The activator bridges the gap, meaning that the electron will de-excite into one of the activators' energy states to produce a smaller x-ray. From the activator energy state, the electron will then de-excite back to the valence band. These x-rays given off cannot excite other electrons because the energy will

be lower than that of the excitation energy, essentially removing the probability of self-absorption.

Organic crystals function on the excitation of electrons on a molecular level, allowing for a faster count rate to be counted. The advantages of organic crystals are that it can be used when faster count rates are needed, and it can be dissolved into a liquid. Inorganic crystals are generally used for nuclear physics experiments because of good energy resolution.

The x-rays interact with the photomultiplier, converting x-rays to free electrons which in turn, hit a dynode. These then cause secondary electrons, which are multiplied and amplified, then sent to the amplifier for further amplification.

The photomultiplier is used to turn the x-ray energy into a usable electrical signal. This process is done in a photosensitive layer, which converts the photons into electrons. Then these electrons are multiplied into a usable signal.

With the multi-channel analyzer, the distribution of energy deposited in the detector can be determined, allowing the one detector to identify pulses of varying degrees and plot them at the same time. These plots will have special characteristics, such as a Compton edge, full energy peak, and single and double escape peaks. The full energy peak is where all of the energy of the gamma-ray is deposited into the detector. The Compton edge is where the scattered electrons carry their maximum energy. Since the scattered electrons can carry different energies depending on the amount of energy deposited by the γ -ray, their energies will be spread throughout the graph, with the Compton edge being the drop off where the

electrons cannot achieve a higher energy from the gamma-rays. The last characteristic is the single and double escape peaks. When a photon with energy above 1.022MeV enters the detector, it can interact with the crystal and form pair production. In this case, all of the energy of the energy would be absorbed by the crystal except for the 1.022MeV. When the positron slows and annihilates, it creates two .511MeV photons, which will either interact within the detector, or escape. If they both escape, then the energy of the γ -ray minus 1.022MeV is detected. If one escapes, then the energy of the γ -ray minus .511MeV is detected. If neither escapes, then the full amount of energy will be deposited within the detector and a reading of the full energy will be given. These conditions where one or both of the photons leaves the detector, cause the single or double escape peak. Figure 2 below shows a typical detector response for the case of energy higher than 1.022 MeV (Knoll, 2000).

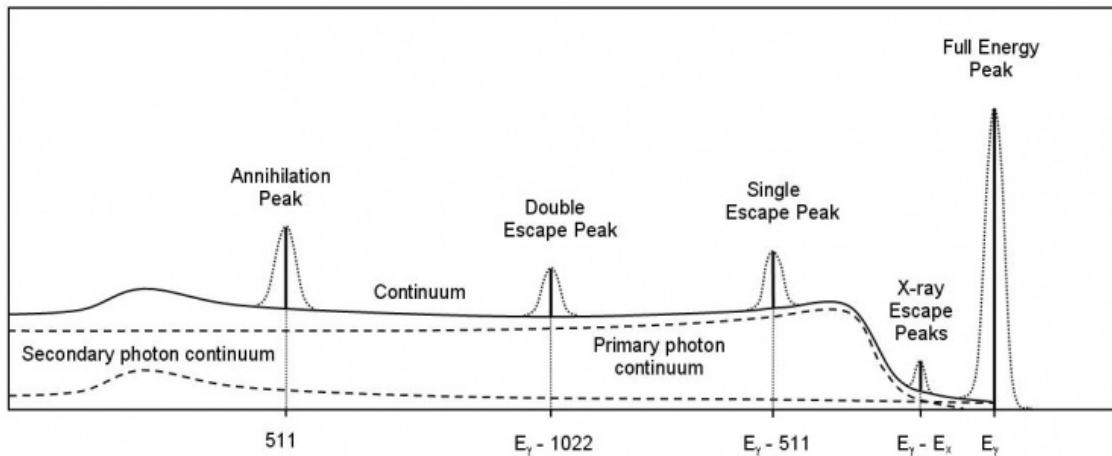


Figure 2: Detector Response

1.3 Alternative Uses

Since its uses in the 1960's and 1970's in Nuclear Engineering, Spectrum Stripping has also been used in a variety of other applications. One of the applications associated with Spectrum Stripping was the study of mechanical relaxation phenomena (Ahmad et. Al, 1971). In this study, there were several overlapping peaks where the analysis proved to be difficult. Figure 3 below shows the relaxation peaks observed in the experiment. Three methods of analysis existed in this study: Spectrum Stripping, Iterative Linear Least Squares, and Iteration of the Gauss method. The study showed that alternative methods were better at determining the contribution of each part to the entire spectrum.

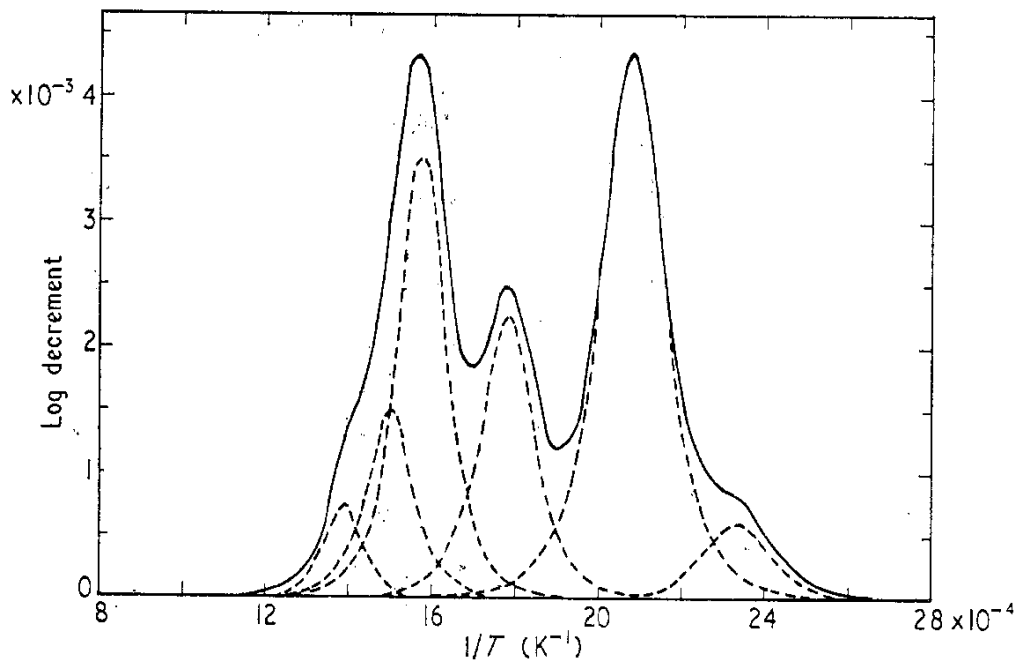


Figure 3: Relaxation Peaks in Ahmad et. Al Experiment

In another study on Photoelectron Spectrum of the Dimethyl Ether-Hydrogen Chloride Complex, Carnovale shows that Spectrum Stripping gives the user a great deal of control over the problem (Carnovale, 1979). In addition, Carnovale states that the use of Spectrum Stripping leaves the residual spectrum with excess noise that should be smoothed with a Gaussian convolution.

In a similar study on Photoelectron Spectrum of Methylenimine by Spectrum Stripping, it is shown that this method by the use of visual assessment is not considered conclusive (Peel, 1975). It is also noted that the spectrum is left with an extreme amount of noise.

1.4 Analysis Involved

The most difficult problem when using the method of Spectrum Stripping is the error analysis. This negative aspect is caused by the error estimated by the user. The only way to accurately measure the error in this case is to relate the values found by successive subtraction to the known contributions. The obvious problem in this is that in any real problem, the actual values should not be known. This is where many people have given up on the use of this method over the years and have only used it to clear unwanted contributions to the spectrum.

Chapter 2

New Spectrum Stripping Analysis

2.1 Reasoning for Method

Over the past four decades, many changes have come about the world. Quite possibly the greatest change in the history of the world has come about from the invention of the computer, allowing people to compute calculations that would have previously taken a lifetime, in a matter of several hours. Another important change during this time frame is the advancement of knowledge in physics. It is for these two reasons that Spectrum Stripping should be reintroduced with modifications that will be discussed later.

There are significant differences in this new method for implementing Spectrum Stripping using computer analysis. One of those differences includes the user no longer needing to graphically remove individual spectra. This means that any error introduced from the graphical technique and user are removed.

2.2 Monte Carlo Simulations

Most of the simulations performed in this study were done using MCNP5, a coding package that has been modified for several decades. As each new addition has been introduced, the accuracy and capabilities of these simulations have positively increased. For each of the three libraries explored in this study a copy of the code used is attached in

Appendices A-C. In addition, each section will have a description of the geometry of the problem and the physics of the individual problem.

The output from MCNP is relatively useless to the user without broadening the output. A Gaussian Broadening code is used to convert the output into a spectrum that matches an experimental spectrum from a given detector size and type. The coefficients used by the Gaussian Broadening code can be changed in order to match those of many different types of detectors. In this study, the coefficients specifically are for a NaI detector.

2.3 Computing Power

The computer simulations from this study were done on the CEAR cluster speeding up the time needed for these simulations. The CEAR cluster consists of 40 AMD Phenom quad-core computing nodes. The processors on each node operate at 2.6 GHz and have 4 Giga Bytes of RAM available to them. It runs on a Linux based operating system in 64 Bit Mode. Figure 4 below is a picture of the cluster.



Figure 4: CEAR Computer Cluster

2.4 Methods of Analysis

In this study, all of the data used for analysis is created from the simulated data. In order to create experimental data, Poisson Statistics is used. A combination of each of the libraries is added together in order to create a simulated experimental spectrum. This is shown in equation 1.

Equation 1: Library Combinations for Experimental Spectrum

$$y_i = A * x_{1i} + B * x_{2i} + \dots N * x_{ni} + \varepsilon_i$$

Where ε_i , is the error in each channel. This is found by first generating a random number between 0 and 1. This is then multiplied by the standard error for Poisson Statistics, commonly known as the square root of the counts. This is shown in equation 2.

Equation 2: Error Equation

$$\varepsilon_i = RN * \sqrt{Counts_i}$$

From here, a modified method for using the Spectrum Stripping technique is used, identifying all of the peaks of interest in the problem. This can be carried out by specifying the channel number or energy associated with the beginning and end of a peak of interest. A Chi-Squared analysis is used to find the best fit for that energy peak, using the simulated libraries for the search. This is then subtracted from the entire spectrum and a residual spectrum is output repeating until the contribution of each library is found. It should also be noted that the lower the Chi-Squared value, the better the fit to the data. The equation used to find the Chi-Squared value is shown in equation 3.

Equation 3: Chi-Squared Test

$$\chi^2 = \sum_{i=1}^n \frac{(y_{icalc} - y_{iknown})^2}{y_{iknown}}$$

With any method used, errors are often found and should be examined when investigating a researching data. The contribution of each library to the total spectrum has an associated error. The error in the entire spectrum is found to accumulate, leading to a higher error than linear least squares (Guo, 2003). Essentially, the greater number of libraries in the sample, the larger the error will be. This is the major issue with this technique, but it will still be shown to be an effective method.

There are two forms of analysis that can be performed. One, which yields the composition of each of the libraries in the entire spectrum, is similar to using linear least

squares, but contains a greater level of error. Another form of analysis is residual identification, residual calculations of the stripped spectrum, used to identify any missing component to the model. After the energy of this residual is determined, a library associated to this energy is added to a linear least squares search, or fitted to the residual spectrum.

Chapter 3

Masking

In the area of national defense, analysis of nuclear spectra is growing in importance. Currently, there are nuclear detectors set up at many of our nation's borders and ports. One of the greatest issues concerning the current technology is that it is solely based on total counts. This leads to many false positives, slowing down the processing at these ports of entry. One proposed improvement to the current technology is using ASP's or Advanced Spectroscopic Portals. This would involve using NaI detectors and computer algorithms to find the types and amounts of radioisotopes inside a cargo container or vehicle. A picture of one of these ASP's is shown below in figure 5. This section provides a proposed method for detecting Uranium in the presence of other radioisotopes.



Figure 5: Picture of an Advanced Spectroscopic Portal

3.1 Introduction to Masking

Masking is the phenomenon that occurs when radioisotopes of higher energy or intensity are used to “mask” the signal of radioisotopes of lower energy or lower intensity. This can occur by using either a strong radioisotope that will overwhelm the detector, or by obscuring the algorithm’s ability to locate the radioisotope of interest. The radionuclide sources in the cargo or vehicle produce spectra that are linear sums of the individual spectra. It is important to understand that the energy of U-235 is very low in comparison to many common radioisotopes, meaning that by using a strong radioisotope, the signature of Uranium can be hidden from the sample. This will be the study of this chapter.

3.2 Analysis for Problem

The method for this problem is started by making libraries using MCNP5. These can be seen in Appendix A-C. For this problem, libraries are made for U-235, Cs-137, and Co-60. There is no shielding used in this problem. After the output is received from MCNP5, Gaussian broadening is incorporated in generating data similar to that from a NaI detector. Figures 6-8 below show the original and broadened data for Cs-137, Co-60, and U-235.

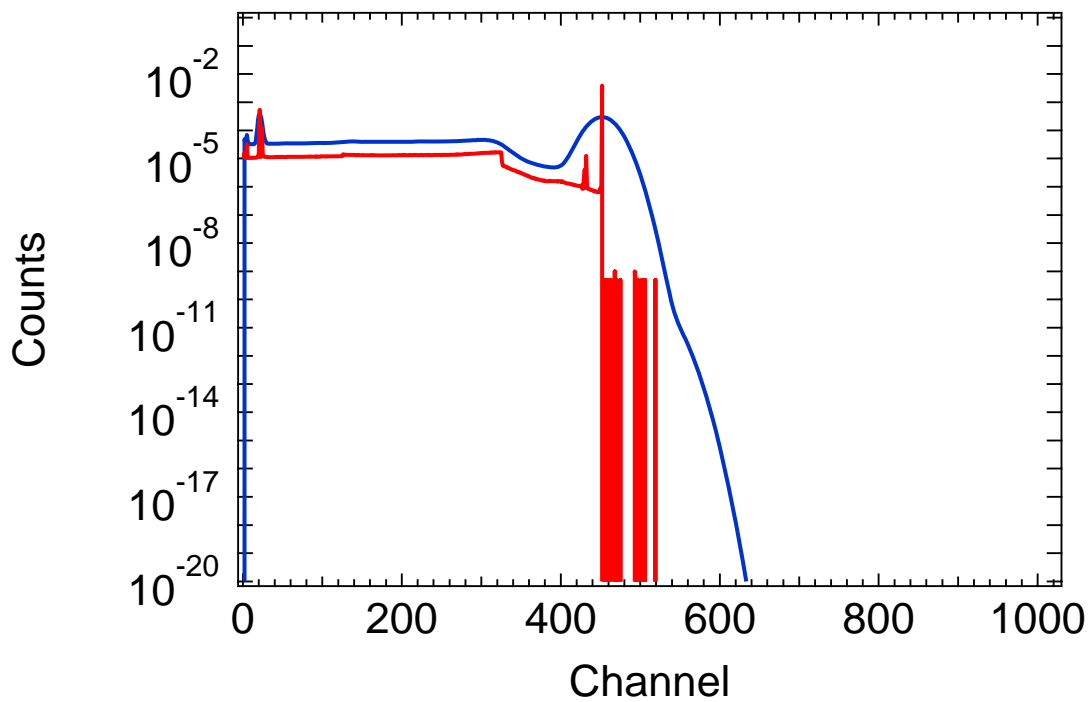


Figure 6: Cs-137 Output from MCNP Original Data and Spread Data

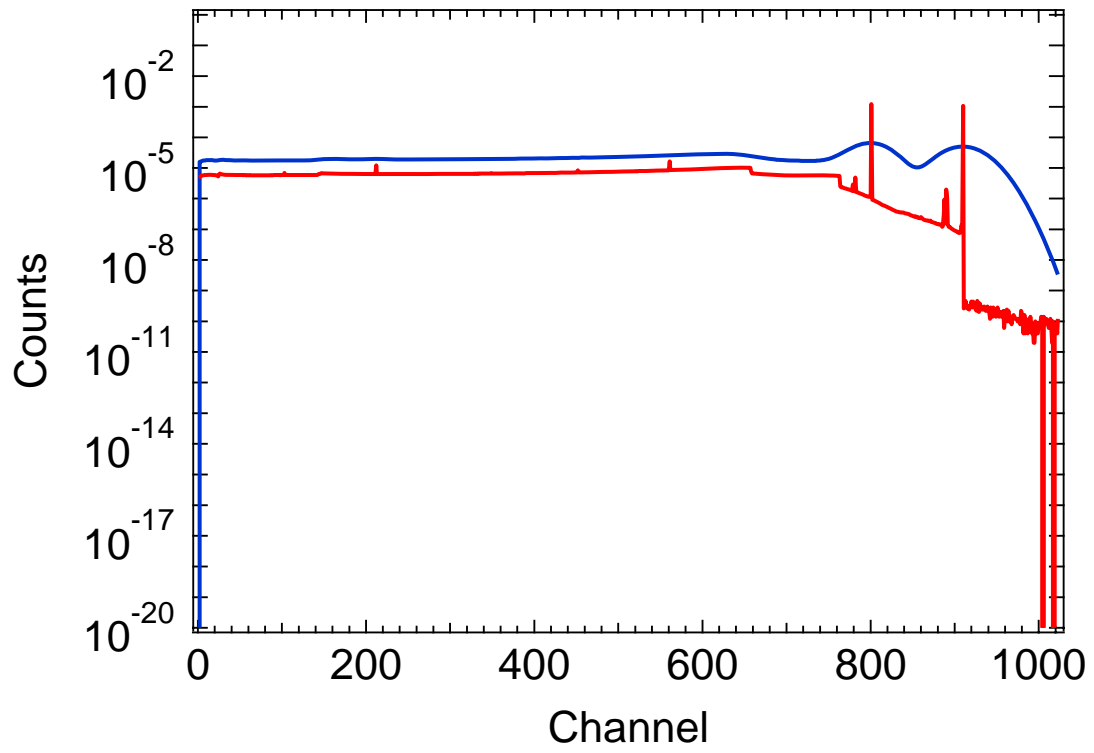


Figure 7: Co-60 Output from MCNP Original Data and Spread Data

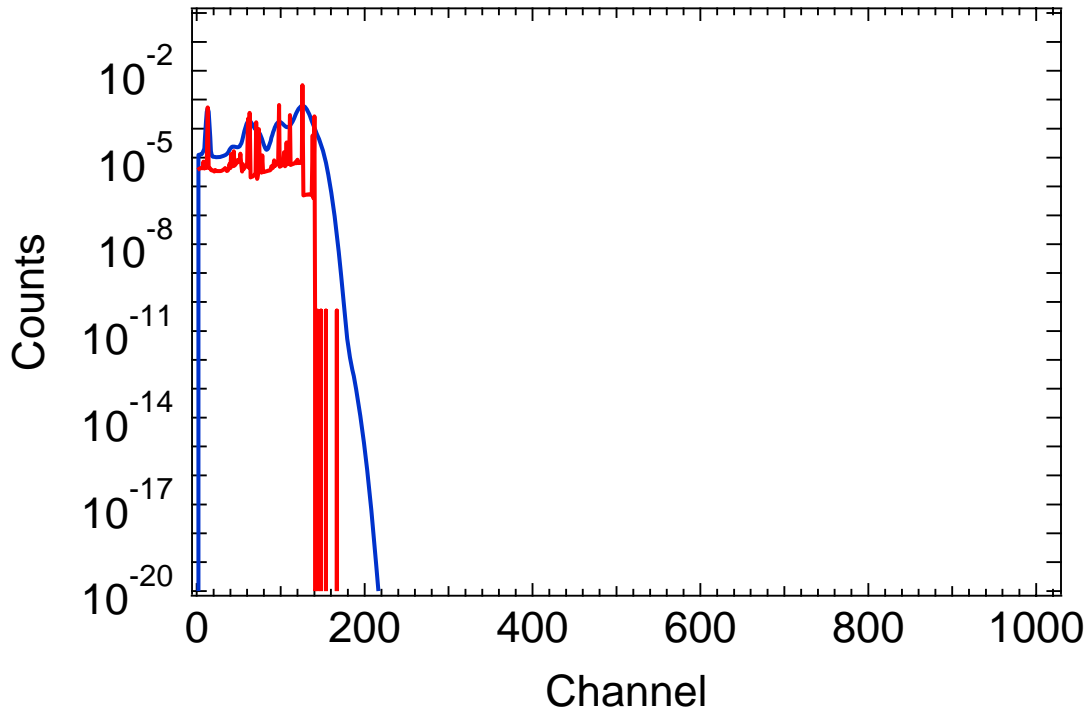


Figure 8: U-235 Output from MCNP Original Data and Spread Data

After this data has been broadened, a linear combination of these radioisotopes is selected. In this analysis, two different amounts are used: one to simulate a situation where there is a high amount of U-235, and another where there is far less than the others. After taking linear combinations of each of these, Poisson Statistics is applied to the spectra in order to randomize the sample to mimic experimental data. From here, a search is performed using Co-60 and Cs-137. The residuals are then shown and analysis is performed on the remaining U-235 in the sample.

3.3 Results

The first case that is explored is the case where the U-235 contribution to the entire spectrum is rather small. For this situation, the linear combinations used for each radioisotope is shown below in table 1. These were chosen to simulate a situation where there is a high counting rate for improved statistics. Figure 9 shows the relative contributions of each radioisotope which are summed to yield Figure 10.

Table 1: Linear Combination of Radioisotopes for Low U-235 Case

| Radioisotope | Linear Contribution |
|--------------|---------------------|
| Co-60 | 1.00E+08 |
| Cs-137 | 1.00E+10 |
| U-235 | 1.00E+07 |

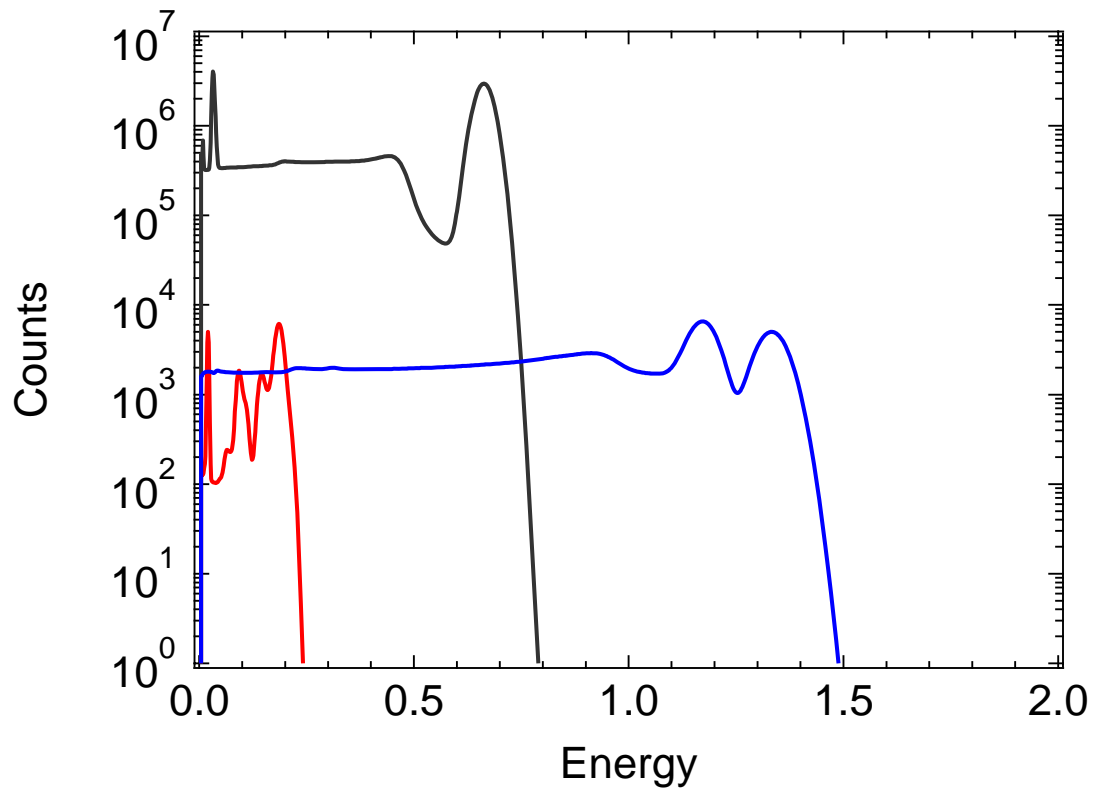


Figure 9: Library Contribution to the Entire Spectrum

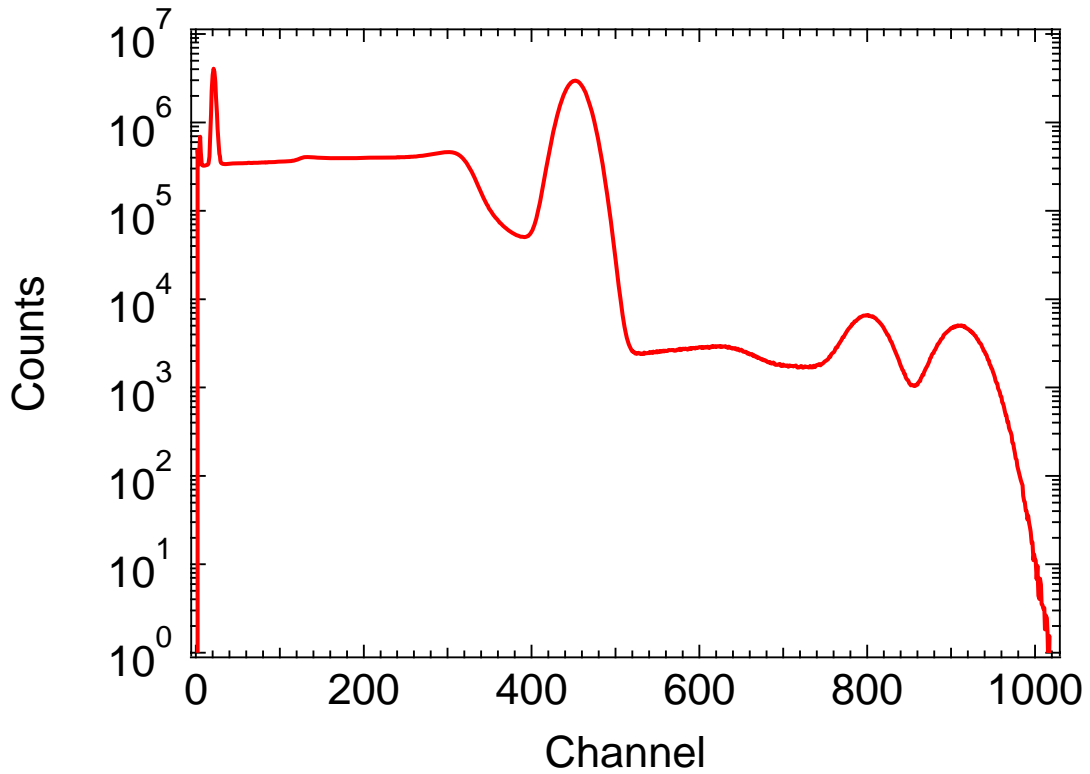


Figure 10: Experimental Spectrum for Limited U-235 Case

After interpreting the data shown in figure 10, the contribution of U-235 cannot be found from visual observation, implying that a screener at a portal monitor would be unable to see any U-235 in this sample.

Next, the libraries for Cs-137 and Co-60 are stripped from the total spectrum. The result is shown as figure 11. This figure shows a close fit to the data from visual observation. The residual calculation reveals that there is a significant difference in the fit as shown in figure 12.

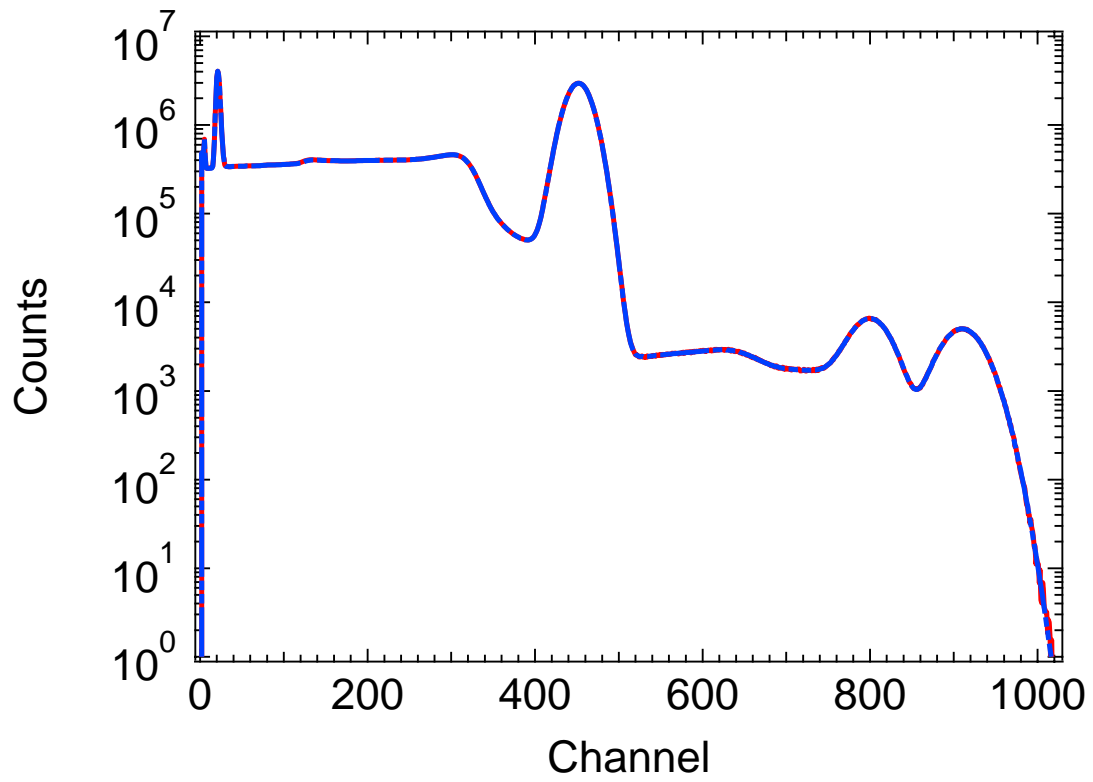


Figure 11: Experimental Spectrum and Fit

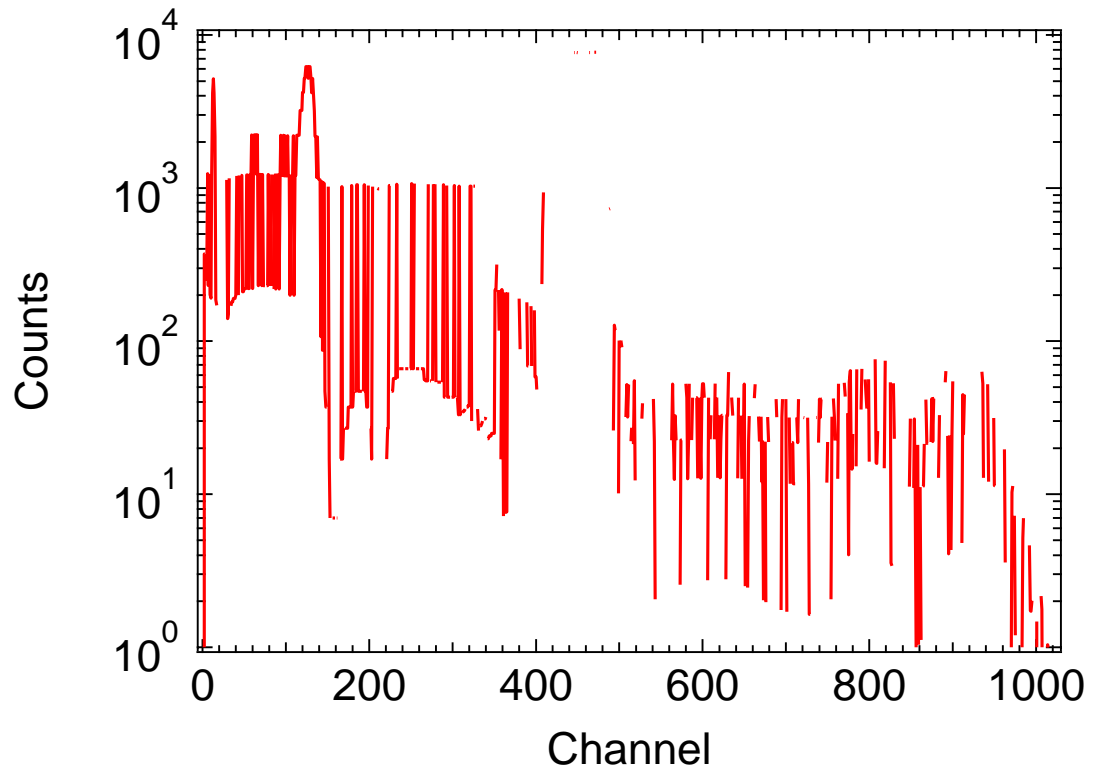


Figure 12: Residuals for Fit

At this point, it is obvious that there is a library missing from the model. After identifying the missing library as U-235, a least squares search can be performed to find the correlation coefficient for U-235. Figure 13 is the best fit for this data.

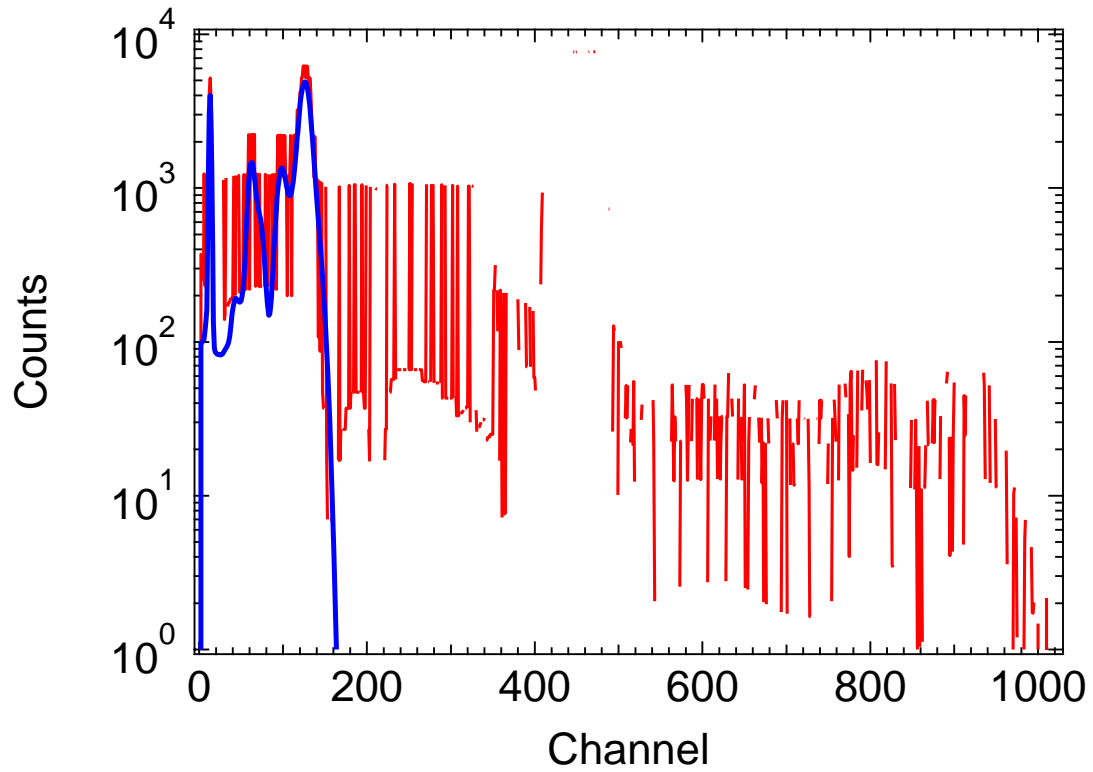


Figure 13: Best Fit for Residual

The calculated linear coefficients by using this technique are shown below in table 2 along with the actual values.

Table 2: Comparison of Results

| Radioisotope | Linear Contribution | Calculated Values | Relative Error |
|--------------|---------------------|-------------------|----------------|
| Co-60 | 1.00E+08 | 9.99E+07 | 0.07% |
| Cs-137 | 1.00E+10 | 1.00E+10 | 0.00% |
| U-235 | 1.00E+07 | 7.89E+06 | 21.06% |

This output can be compared to the results that would come from using linear least squares. Figure 14 shows the original data and fit. The result is not visually different from the fit using Spectrum Stripping. Figure 15 shows the residuals, which shows a noticeable difference between these two methods.

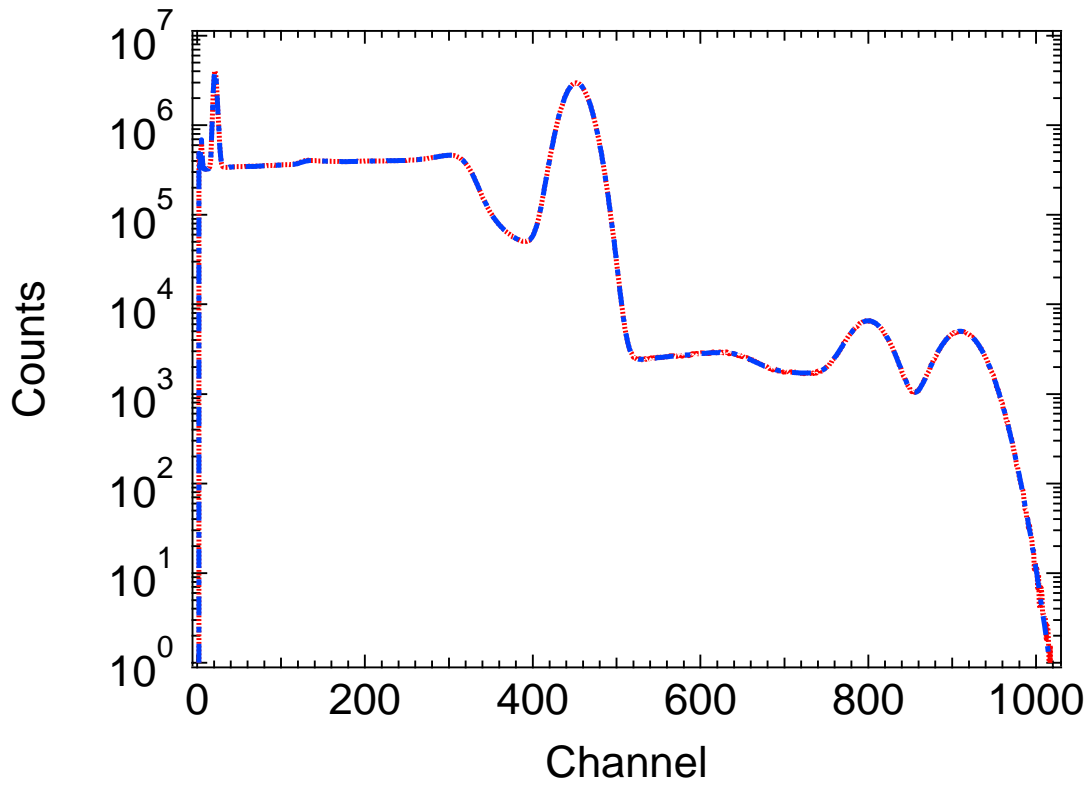


Figure 14: Fit Using Linear Least Squares

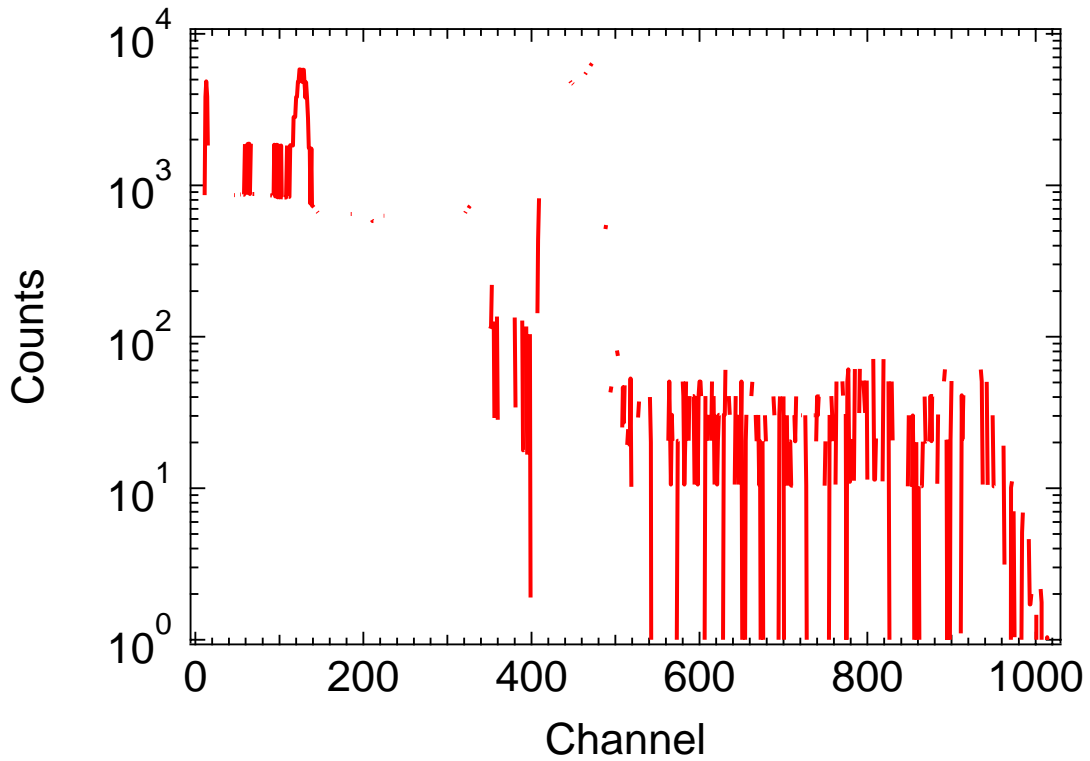


Figure 15: Residuals Using Linear Least Squares Method

The resulting identification a U-235 signature would prove to be difficult, since the peaks are hard to distinguish. This is due to an inherent overshoot that occurs while using linear least squares. This is more apparent in limiting cases such as the low U-235 case. In the case where there is a large amount of U-235, this problem will be less apparent.

The next consideration is the case where there is a large contribution from U-235, using the same analysis from the previous case, Table 3 below lists the new linear coefficients used for this case. The total spectrum is shown as figure 14.

Table 3: Linear Coefficients for High U-235 Case

| Radioisotope | Linear Contribution |
|--------------|---------------------|
| Co-60 | 1.00E+08 |
| Cs-137 | 1.00E+08 |
| U-235 | 1.00E+10 |

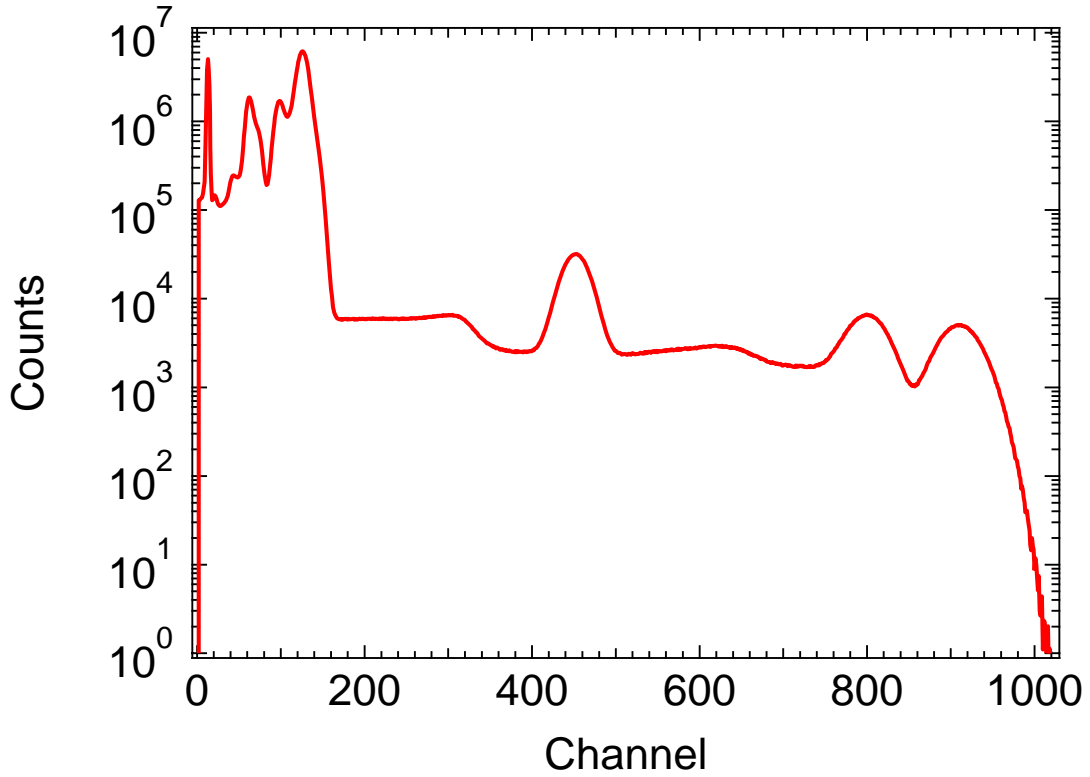


Figure 16: Experimental Spectrum for High U-235 Case

In the same manner as the previous case, the Co-60 and Cs-137 are stripped from the entire spectrum. Figure 15 shows the amount being stripped from the sample. The residual is shown in figure 16 and the best fit is shown in figure 17. The calculated linear coefficients and a comparison to the original data are listed in table 4.

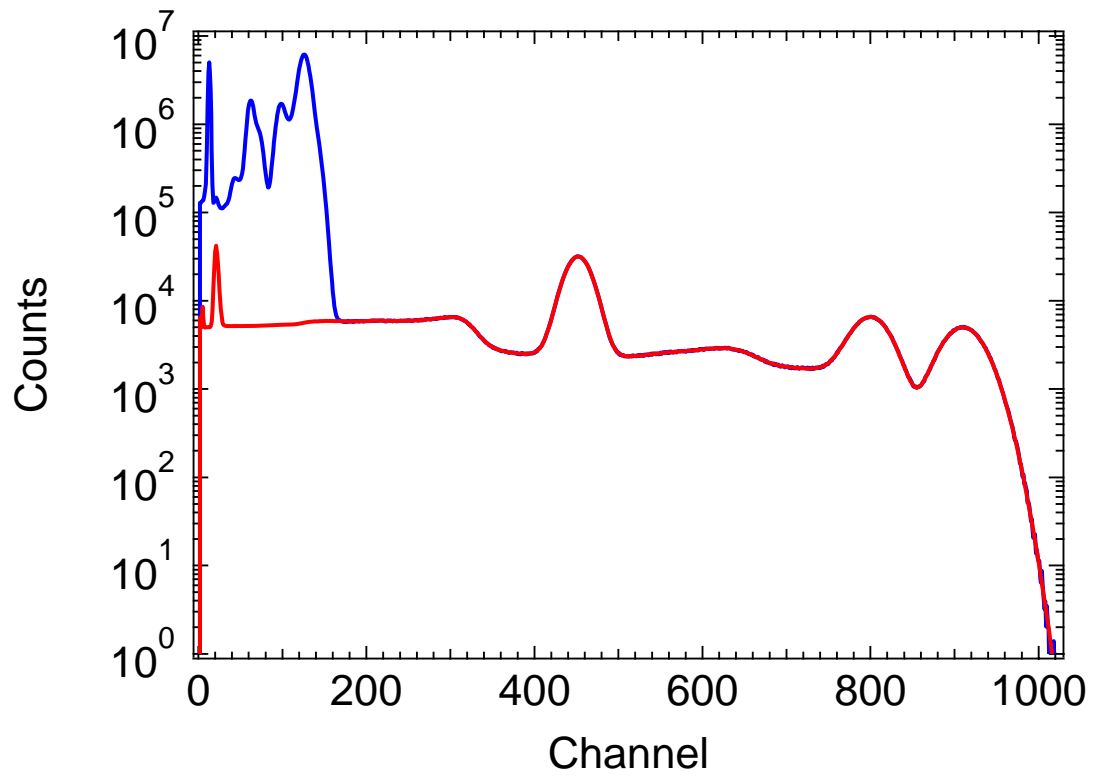


Figure 17: Original Data and Fit for High U-235 Case

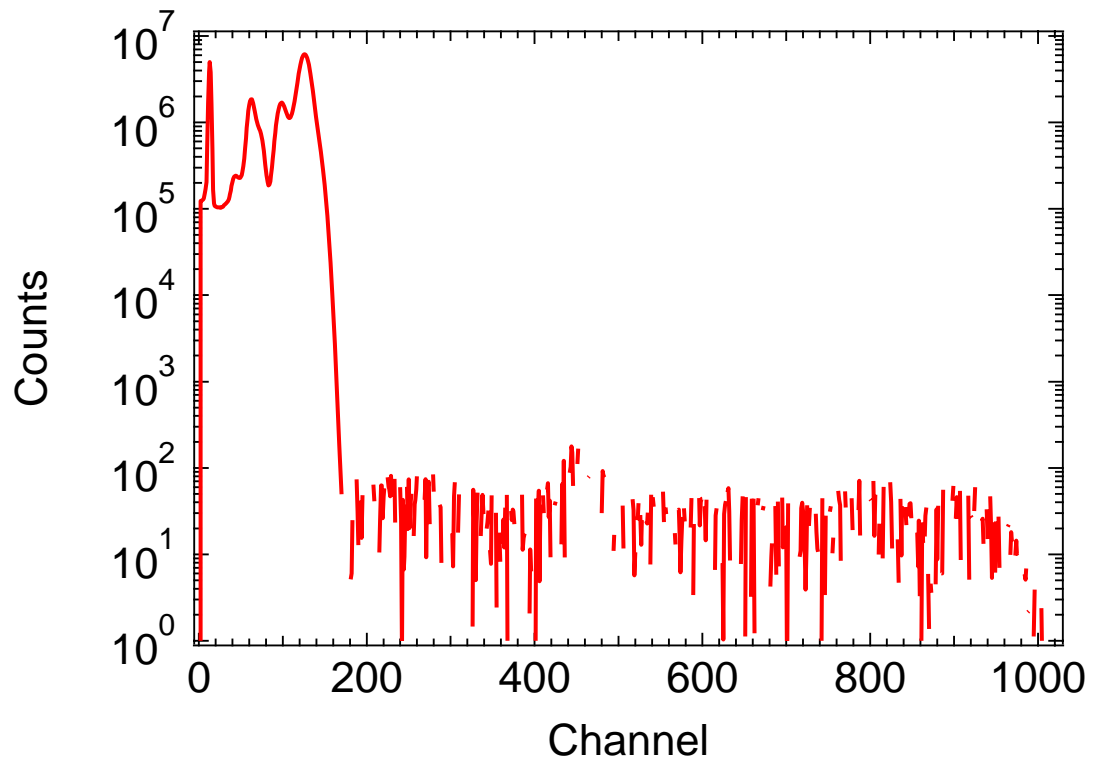


Figure 18: Residual for High U-235 Case

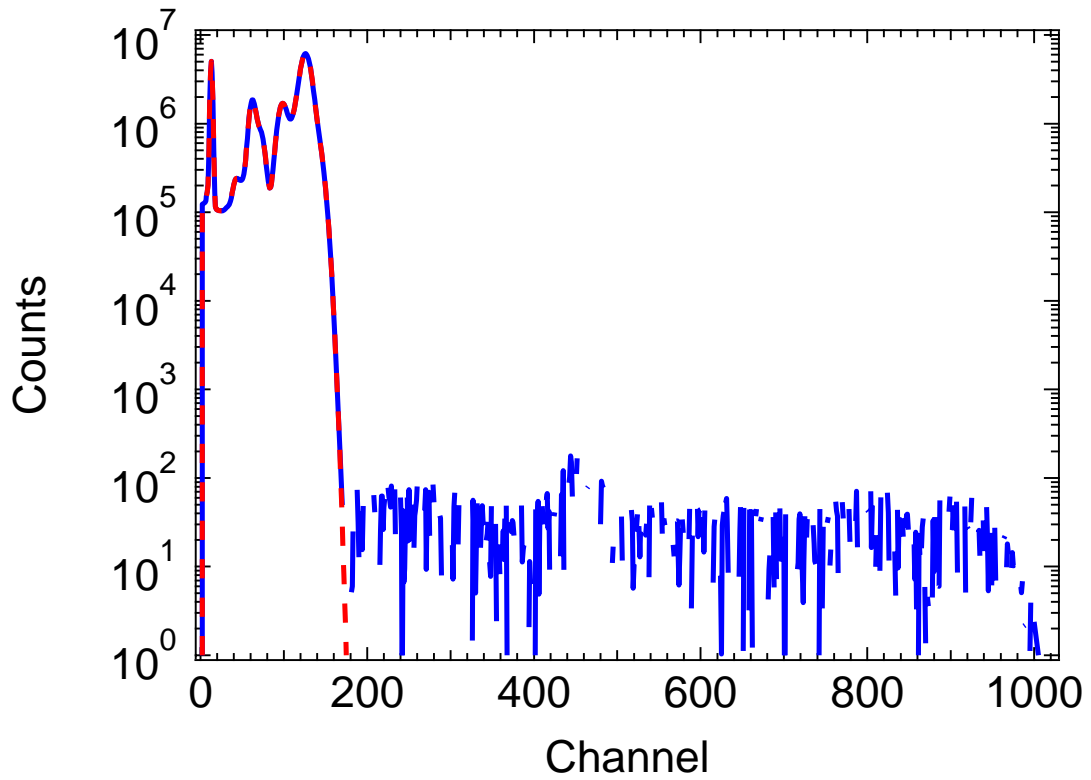


Figure 19: Best Fit for the Residual Calculation

Table 4: Comparison between Experiment and Calculated Values

| Radioisotope | Linear Contribution | Calculated Values | Relative Error |
|--------------|---------------------|-------------------|----------------|
| Co-60 | 1.00E+08 | 9.998E+07 | 0.02% |
| Cs-137 | 1.00E+08 | 9.997E+07 | 0.03% |
| U-235 | 1.00E+10 | 9.999E+09 | 0.01% |

Chapter 4

Phase Samples

Another difficult problem is maintaining an online system of analyzing bulk flow through an oil pipe. One proposed method is to use Prompt Gamma Neutron Activation Analysis (PGNAA). PGNAA can be used in many applications and can also be used for detecting anything from grams to micrograms. It is a non-destructive method; therefore, it can be used without causing any damage to the sample or equipment surrounding the sample. Each sample takes from a few minutes to several hours to get suitable counting statistics.

PGNAA is performed by continuously irradiating a sample with a beam of neutrons. Each nucleus (other than that of He-4) emits a prompt gamma ray after absorbing a neutron. Each nucleus gives off different energy signatures that can be identified using gamma-ray spectrometers, while their concentrations can be identified by the intensities of these peaks.

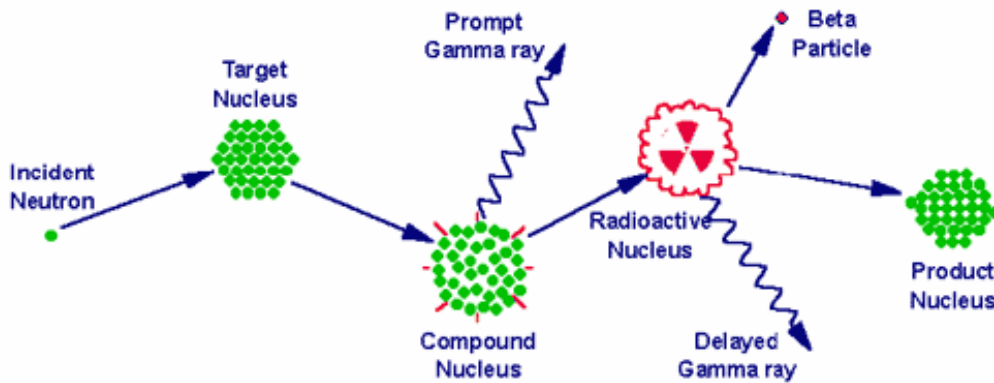


Figure 20: Visual of Prompt Gamma Neutron Activation Analysis

4.1 Introduction to CEARCPG

The libraries used for this analysis are generated by using a code developed by the Center for Engineering Applications of Radioisotopes (CEAR) called CEARCPG. CEARCPG is a specific purpose Monte Carlo code used for PGNAA simulations. Instead of using individual radioisotopes for analysis, phase libraries are created. These phase libraries are the expected makeup of specific phases of the bulk flow. For instance, a phase library for gas would be made up of the natural gas that would be found in a natural gas deposit. For this analysis, three phase libraries are considered: Salt, water, and air. Figures 21-23 display these three phase libraries.

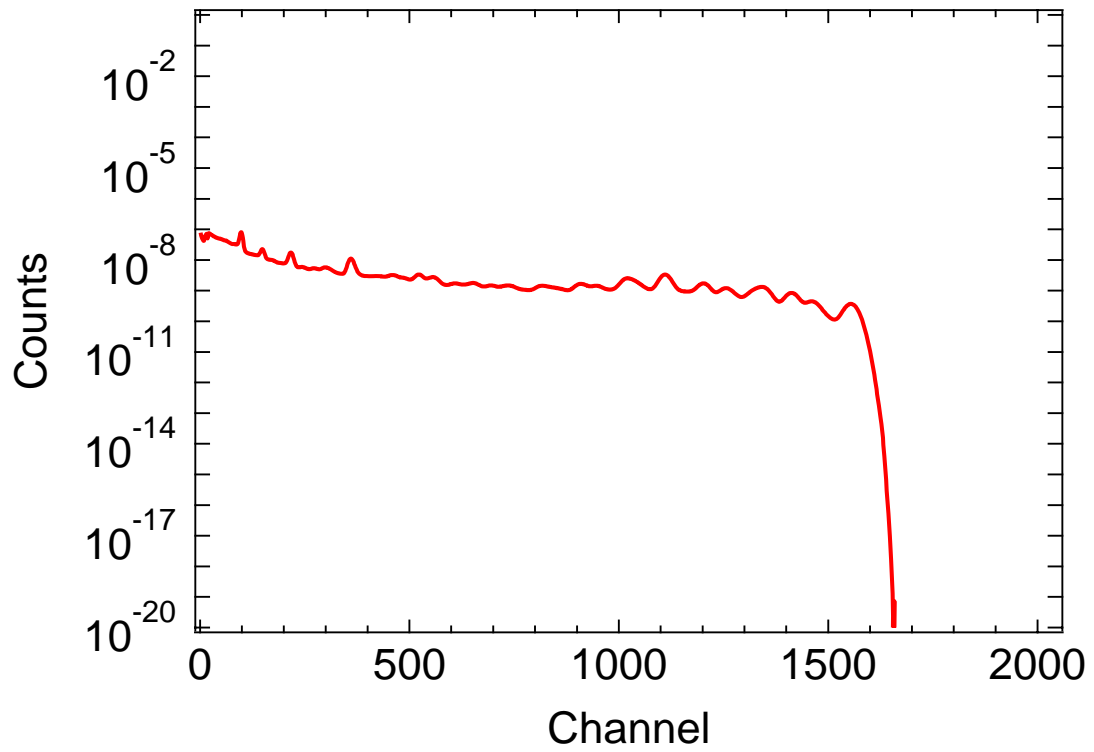


Figure 21: CEARCPG Output for Salt Library

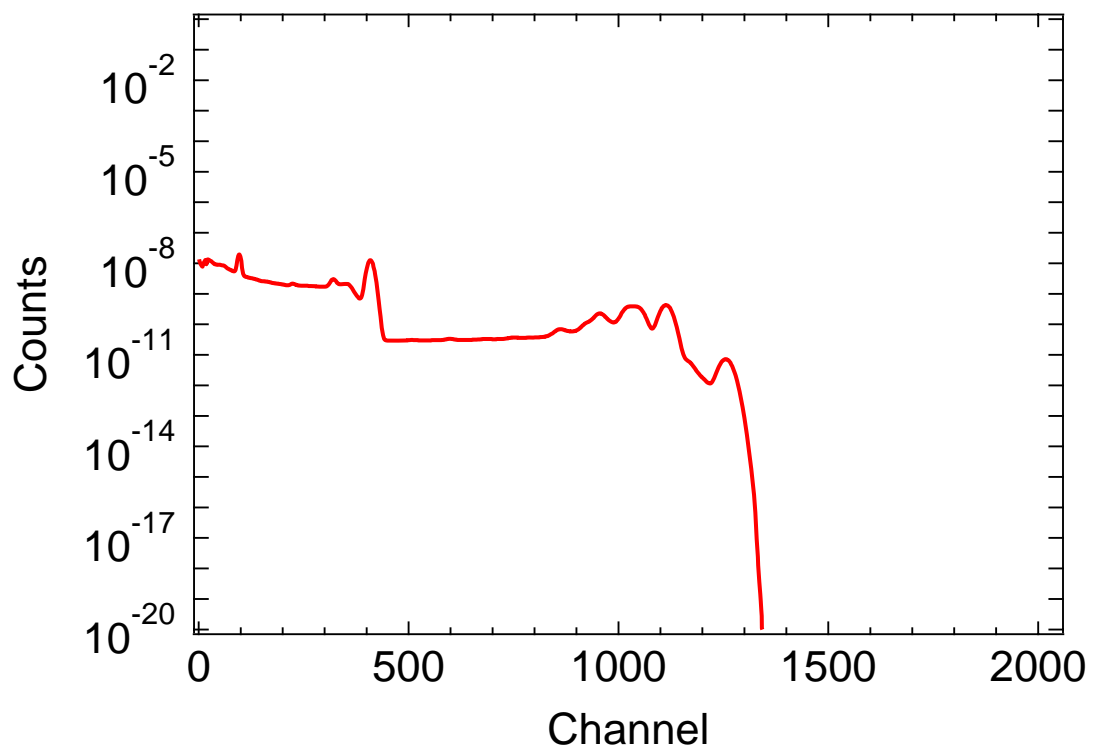


Figure 22: CEARCPG Output for Water Library

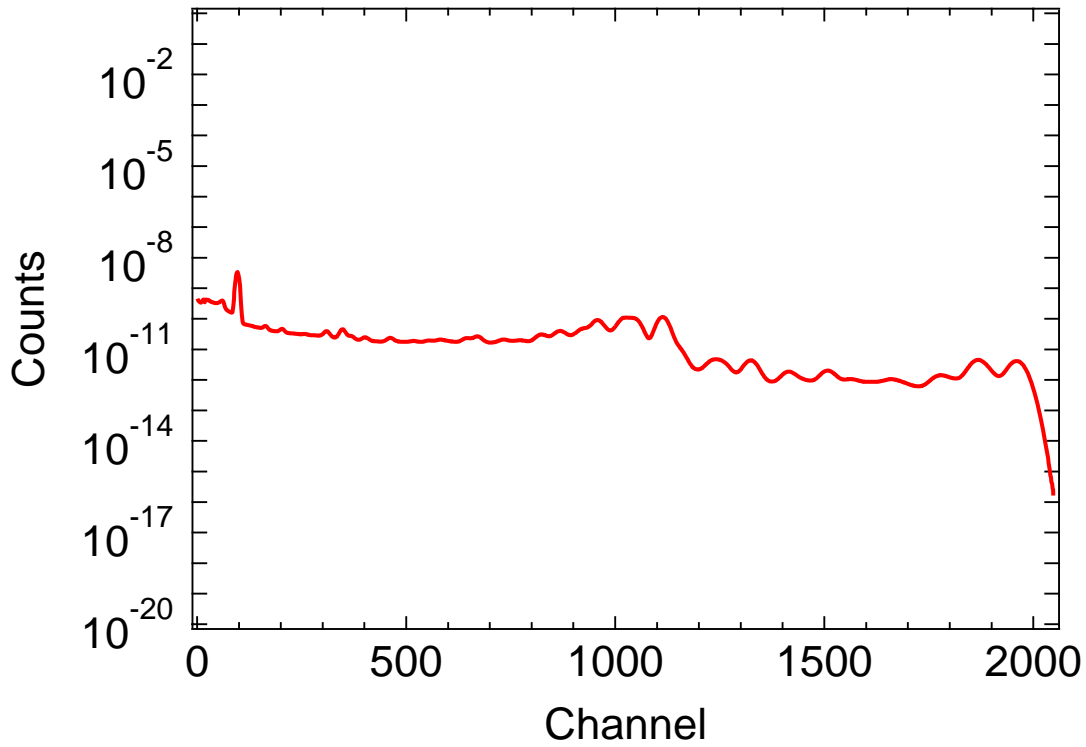


Figure 23: CEARCPG Output for Air Library

4.2 Analysis

The method for preparing this problem is similar to the method used in the previous case. Linear combinations of the pre-generated phase libraries are added to create an experimental spectrum, after Poisson Statistics are used. Then, the sample is ready for analysis by stripping individual spectra, leaving residuals. Even though this analysis is better than linear least squares, it is necessary to understand that searching on peak areas will prevent an overshoot of the data. This will leave mostly positive residuals, providing for an improved analysis method compared to data that is varied around zero.

4.2 Results

The experimental spectrum is prepared using the libraries for salt, water, and air.

Table 5 lists the linear correlation coefficients used to create the experimental spectrum. The individual libraries and total experimental spectrum are shown below in figures 24 and 25.

Table 5: Linear Correlation Coefficients for Phase Libraries

| Library | Coefficient |
|---------|-------------|
| Salt | 1.00E+14 |
| Water | 1.00E+14 |
| Air | 1.00E+14 |

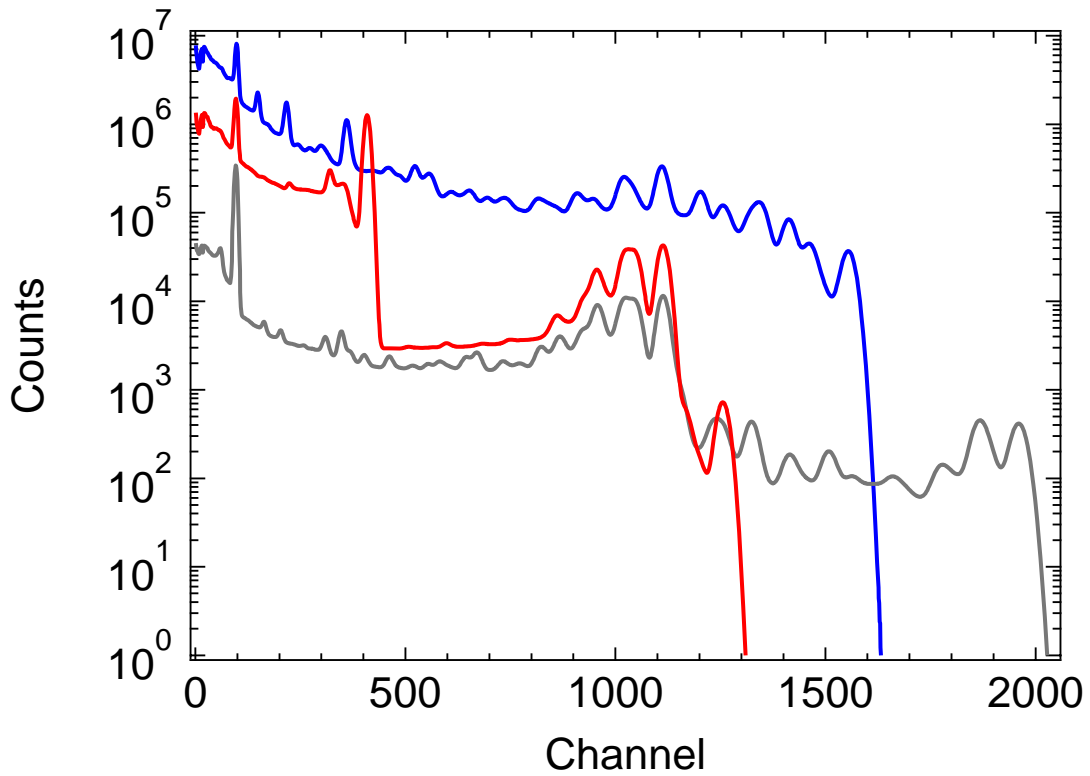


Figure 24: Library Contribution to Experimental Spectrum

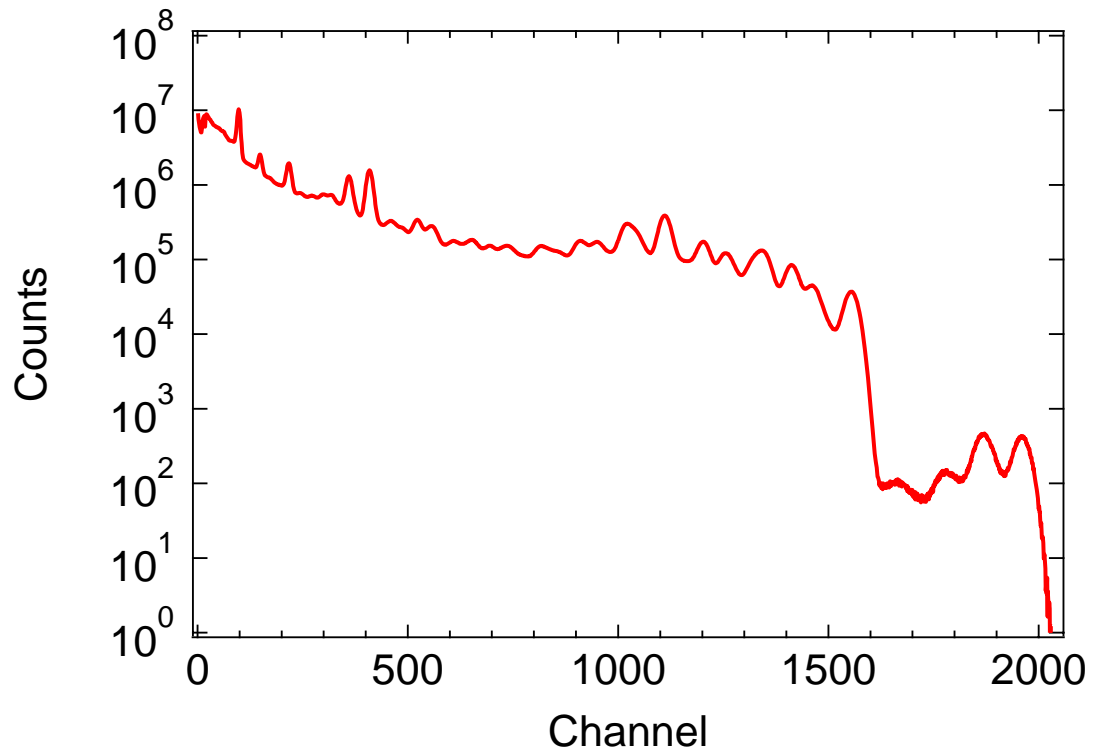


Figure 25: Experimental Spectrum

The highest energy library is subtracted out and is shown in figure 26, with the corresponding residual, figure 27.

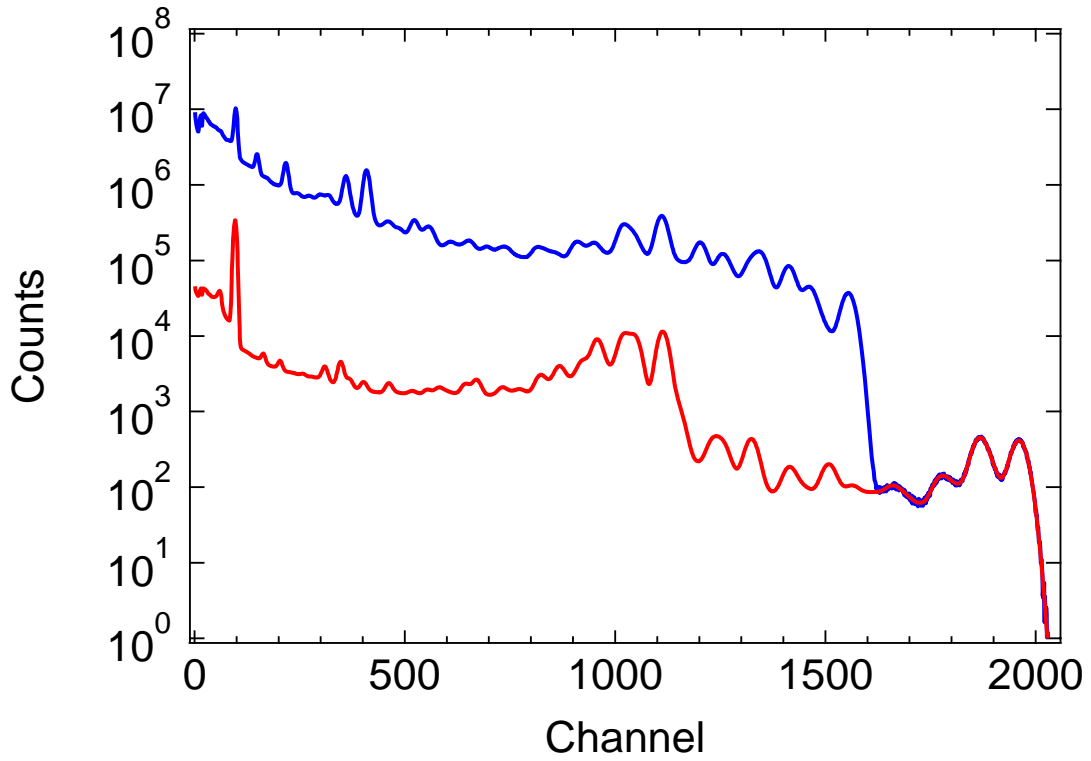


Figure 26: Fitted Data for Air Library

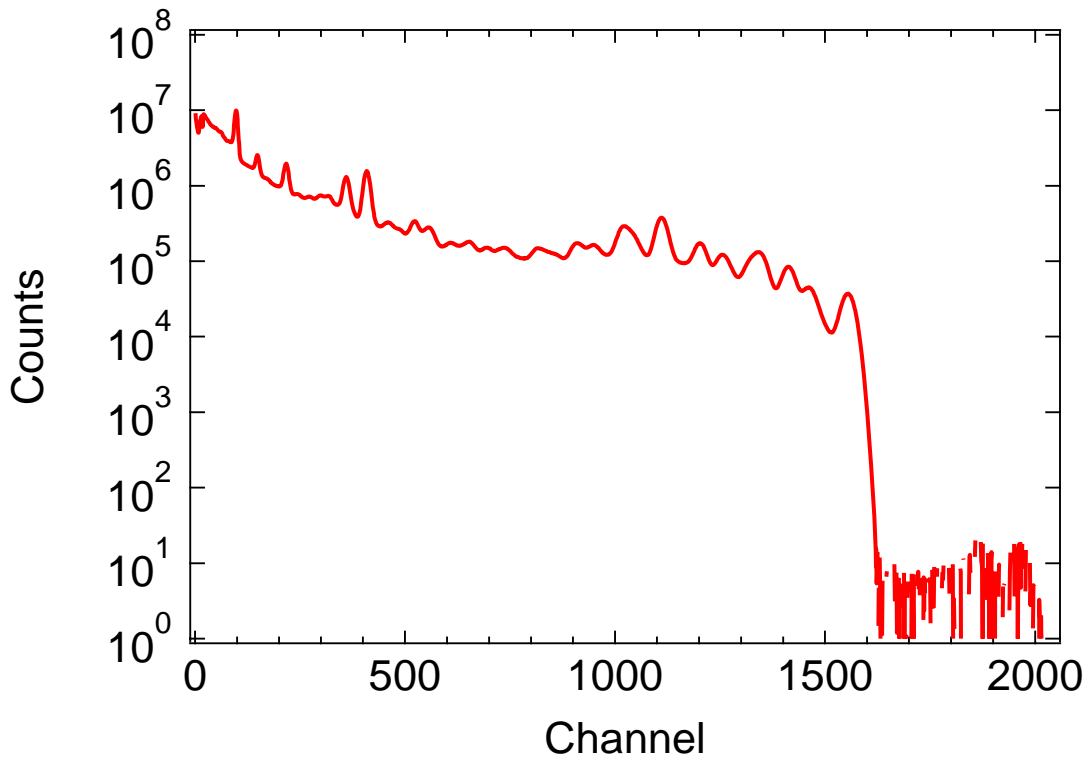


Figure 27: Residual after Removing Air Library

The next highest energy library is that of salt. This library is removed, resulting in figure 28, and the corresponding residual figure 29.

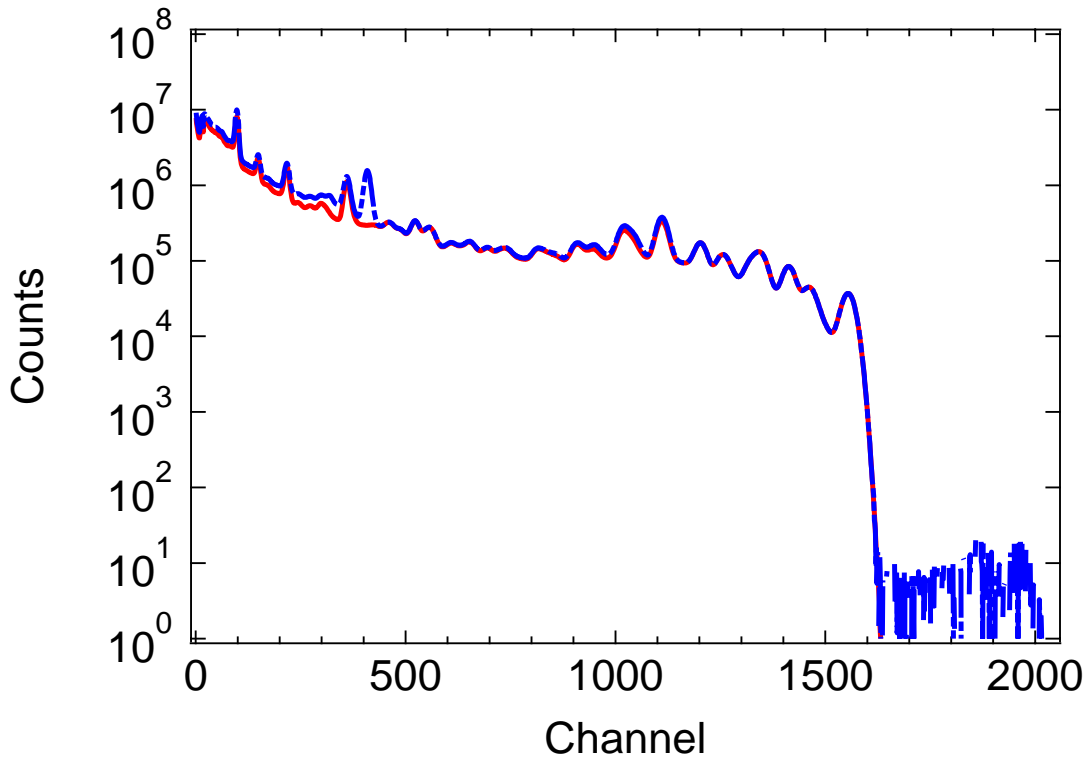


Figure 28: Fitted Data for Salt Library to Residual

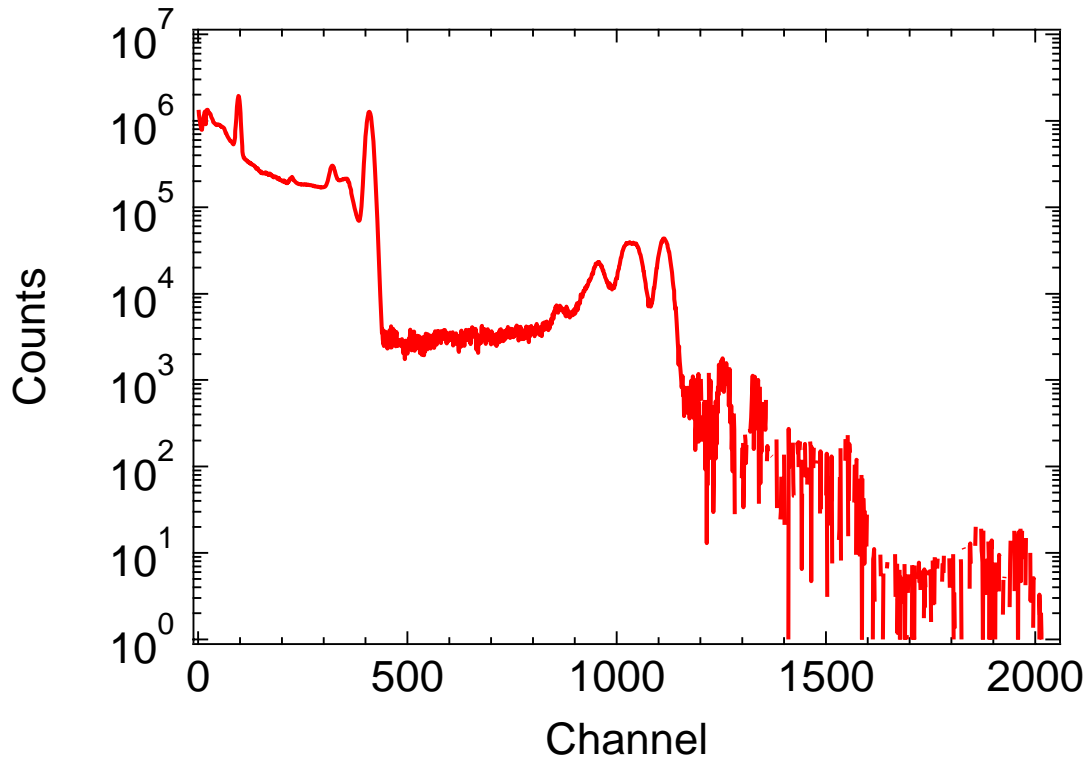


Figure 29: Residual after Removing Salt Library

The resulting residual is then fitted to the water library, which results in figure 30.

The calculated coefficients are compared to the known amounts in table 6.

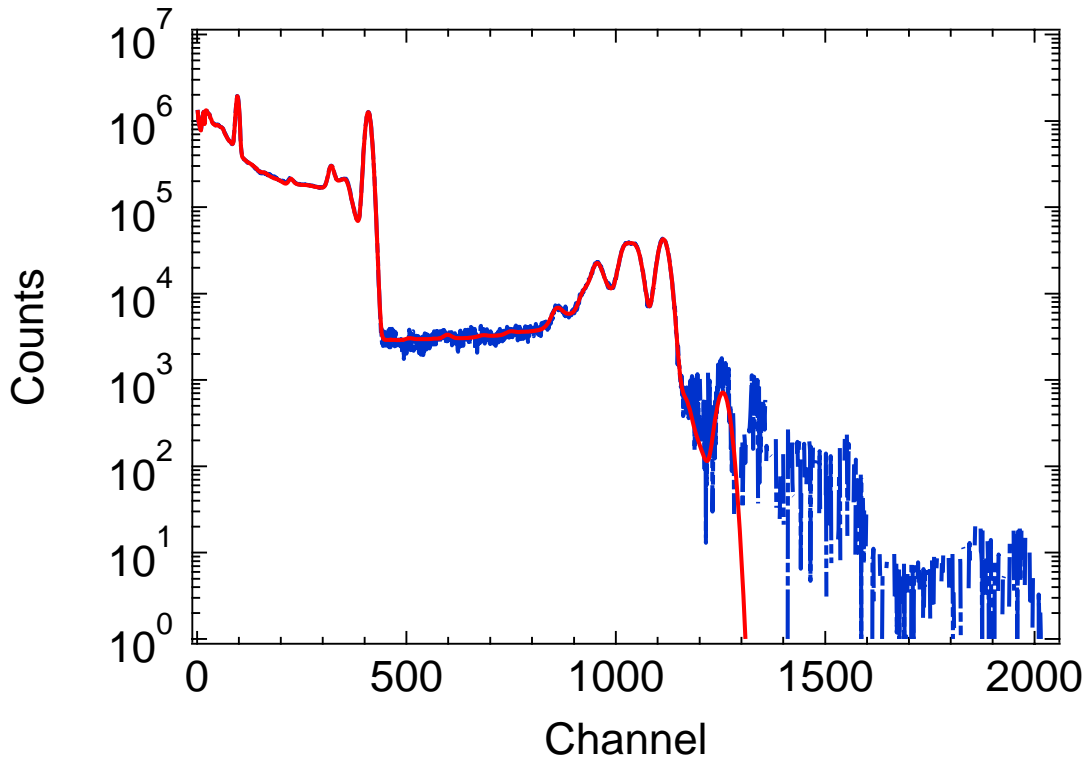


Figure 30: Fitted Data for Water Library to Stripped Spectrum

Table 6: Comparison between Calculated and Known Amounts

| Library | Known Coefficient | Calculated Coefficient | Relative Error |
|---------|-------------------|------------------------|----------------|
| Air | 1.00E+14 | 9.990E+13 | 0.10% |
| Salt | 1.00E+14 | 1.000E+14 | 0.00% |
| Water | 1.00E+14 | 9.924E+13 | 0.76% |

Chapter 5

Discussion

These two applications show the importance of Spectrum Stripping. There are inherent problems in using library linear least squares method for situations where not all libraries are known. By simply stripping these libraries away, the user can avoid an overshoot of the data. The result of this is greater accuracy in the subsequent calculations on the residuals. The error does accumulate based on propagation of errors, but the overall solution is more accurate when compared to the known values.

There are several applications that have been explored, not included in this study, that show this method has some areas of weakness. In situations where specific peaks can not be searched on, such as convoluted peaks, spectrum stripping does not produce results that are accurate. The results change severely based on the area of searching, and any minor change can result in large differences in the residual calculations. In any method that is to become fully automated, these types of effects should be avoided at all costs.

One major improvement over the old method of Spectrum Stripping is that there is no longer subjectivity in the user. However, the user must have a large amount of insight into the problem in order to produce accurate simulations and choose the correct libraries to include in the analysis of the data.

The libraries and data in this study are entirely pre-calculated and simulated. In a real world situation, there are other measures that would need to be taken in order to analyze the

data. For any case where there is a lot of inherent noise, a smoothing function should be utilized. This can also be useful in situations where there is a low counting rate. This will add a significant amount of error, but should provide higher accuracy. Several other programs should be utilized in order to shift a spectrum to account for changes in linearity, creep in the voltage, and differences in detection systems. The Center for Engineering Applications of Radioisotopes has a GShift FORTRAN based code that can handle all of these problems. Another program that can be utilized is the Peaks program that can identify peaks in a system.

Chapter 6

Future Work

One of the most important problems that Spectrum Stripping can be applied to is identifying the background in a cargo monitoring situation. Cargo monitoring is a difficult problem that is being worked on at many of the national laboratories throughout the United States. This problem is rather difficult, because there are many factors that are constantly changing. To begin with, there is natural background at all times. This can be found by setting up a simple detector. As a shipping crate is introduced to the system, the crate will actually shield the detector from background radiation. This will result in a drop in background counts. If there is anything within the crate that is radioactive, then the detector will be able to pick this up. There are possible scenarios in which there could be radioactive material in the crate that may go unnoticed, because the crate will lower the background more than the detector will receive a signal from the radioactive material.

The other difficult challenge in this problem comes from the generation of libraries to begin a search with. The physics of the problem becomes increasingly difficult as soon as shielding material is considered. There is no longer a simple simulation in which a particle is detected in the way described earlier in this study. There are now interactions that are taking place before the particle ever reaches the detector. This will drastically change the detector response. Heavier shield materials such as lead will have a high absorption probability,

leading to a reduced number of particles reaching the detector. This will result in identifying a lower amount of radioactive material than is actually present. Shielding materials with a lower atomic number tend to have more scattering. This will lower the energy of the incoming particle, which will ruin any algorithm's attempt to determine the identity and amount of the radioactive material.

It is this author's opinion that Spectrum Stripping should be used in this case to remove known elements from the entire spectrum. Even if not all of the radioisotopes or shielding materials are known, the removal of the elements that are known will make the problem much easier to solve.

Chapter 7

Conclusions

This study has shown that there are some inherent issues with using the linear least squares method in situations where not every library is known. The linear least squares method will overshoot the data, resulting in residuals that are difficult to analyze. This problem has been solved by revisiting the old method of Spectrum Stripping. Although the error will be higher by using Spectrum Stripping, the results show that Spectrum Stripping will give a more accurate answer to the unknown element. It is for this reason that Spectrum Stripping should be further investigated in nuclear security and oil well logging, as well as other applications outside of this discipline.

REFERENCES

- Ahmad, M.S. et. Al. "Computer Analysis of Complex Relaxation Spectra," J. Phys. D: Appl. Phys. Vol.4 (1971)
- Bevington, P.R. and Robinson, D.K. Data Reduction and Error Analysis for the Physical Sciences. 3rd Edition. United States: McGraw-Hill Higher Education. (2003.)
- Burr, Tom, and Hamada, Michael. "Radio-Isotope Identification Algorithms for NaI γ Spectra," Algorithms (2009.)
- Carnovale, F. et. Al. "The Photoelectron Spectrum of the Dimethyl Ether-Hydrogen Chloride Complex," Journal of the American Chemical Society (1980.)
- Furr, A.K., Robinson, E.L, and Robins, C.H. "A Spectrum Stripping Technique for Qualitative Activation Analysis using Monoenergetic Gamma Spectra," Nuclear Instruments and Methods 66 (1968.)
- Guo, W., Gardner, R.P, and Todd, A.C. "Using the Monte Carlo-Library Least-Squares (MCLLS) approach for the in vivo XRF measurement of lead in bone," Nuclear Instruments and Methods in Physics Research A 516 (2004.)
- Heath, R.L. "Computer Techniques for the Analysis of Gamma-Ray Spectra Obtained with NaI and Lithium-Ion Drifted Germanium Detectors," Nuclear Instruments and Methods 43 (1996.)
- Knoll, Glenn F. Radiation Detection and Measurement. 3rd ed. United States: John Wiley & Sons, Inc. (2000.)
- Peel, J.B., and Willett, G.D. "Photoelectron Spectrum of Methylenimine by Spectrum Stripping," J. Chem. Soc., Faraday Trans. 2 (1975.)
- Salmon, L. "Analysis of Gamma-Ray Scintillation Spectra by the Method of Least Squares," Nuclear Instruments and Methods 14 (1961.)

APPENDIX

APPENDIX A: U-235 MCNP INPUT DECK

2x2 NaI Detector

c

c Cell Card

c

c Detector

14 4 -2.7 31 -23 -28 29
15 4 -2.7 -23 -4 28
16 5 -3.67 -30 -33 29
17 6 -2 -31 -28 32
18 7 -2.2 -31 30 -32 29
19 7 -2.2 -30 -32 33

c

c Voids

99998 0 -100 #14 #15 #16 #17 #18 #19
99999 0 100

c Surface Card

c Detector

4 px 8
23 c/x 0 11.6 2.74828
26 c/x 0 11.6 2.740919999
28 px 7.9492
29 px 0.05615
30 c/x 0 11.6 2.54
31 c/x 0 11.6 2.69748
32 px 7.79172
33 px 7.74092

c

c Box For Inside Void

100 rpp -45 45 -15 15 -5 30

mode p e

c

c Materials

m4 12000. -0.01 \$ Aluminum (6061-T6)
13000. -0.9715 14000. -0.005 22000. -0.001
24000. -0.002 25000. -0.001 26000. -0.005
29000. -0.0025 30000. -0.002
m5 11000. -0.15307 \$ NaI(Ti) p= 3.67
53000. -0.8457 81000. -0.00123

```
m6 14000.      -1 $ Padding
m7 6000.04p    2 $ Reflector
   9000.04p     4
c
c Data Card
imp:p 1 1 1 1 1 1 0
imp:e 1 1 1 1 1 1 0
f8:e 16
e8 0.0 1024i 1.5
sdef par=2 pos=18 0 11.6 erg=D1
c U-235
si1 L 0.013 0.01959 0.089953 0.09335 0.105 0.10916 0.14376 0.16333 0.185715
    0.20211 0.205311
sp1 D 0.51 0.61 0.0356 0.0581 0.0269 0.0154 0.1096 0.0508 0.572
    0.0108 0.0501
nps 20000000000
```

APPENDIX B: CO-60 MCNP INPUT DECK

2x2 NaI Detector

c

c Cell Card

c

c Detector

14 4 -2.7 31 -23 -28 29

15 4 -2.7 -23 -4 28

16 5 -3.67 -30 -33 29

17 6 -2 -31 -28 32

18 7 -2.2 -31 30 -32 29

19 7 -2.2 -30 -32 33

c

c Voids

99998 0 -100 #14 #15 #16 #17 #18 #19

99999 0 100

c Surface Card

c Detector

4 px 8

23 c/x 0 11.6 2.74828

26 c/x 0 11.6 2.740919999

28 px 7.9492

29 px 0.05615

30 c/x 0 11.6 2.54

31 c/x 0 11.6 2.69748

32 px 7.79172

33 px 7.74092

c

c Box For Inside Void

100 rpp -45 45 -15 15 -5 30

mode p e

c

c Materials

m4 12000. -0.01 \$ Aluminum (6061-T6)

13000. -0.9715 14000. -0.005 22000. -0.001

24000. -0.002 25000. -0.001 26000. -0.005

29000. -0.0025 30000. -0.002

m5 11000. -0.15307 \$ NaI(Ti) p= 3.67

53000. -0.8457 81000. -0.00123

m6 14000. -1 \$ Padding

```
m7 6000.04p      2 $ Reflector
   9000.04p      4
c
c Data Card
imp:p 1 1 1 1 1 1 0
imp:e 1 1 1 1 1 1 0
f8:e 16
e8 0.0 1024i 1.5
sdef par=2 pos=18 0 11.6 erg=D1
si1 L 1.173237 1.332501
sp1 D 0.999736 0.9998561
nps 2000000000
```

APPENDIX C: CS-137 MCNP INPUT DECK

2x2 NaI Detector

c

c Cell Card

c

c Detector

14 4 -2.7 31 -23 -28 29

15 4 -2.7 -23 -4 28

16 5 -3.67 -30 -33 29

17 6 -2 -31 -28 32

18 7 -2.2 -31 30 -32 29

19 7 -2.2 -30 -32 33

c

c Voids

99998 0 -100 #14 #15 #16 #17 #18 #19

99999 0 100

c Surface Card

c Detector

4 px 8

23 c/x 0 11.6 2.74828

26 c/x 0 11.6 2.740919999

28 px 7.9492

29 px 0.05615

30 c/x 0 11.6 2.54

31 c/x 0 11.6 2.69748

32 px 7.79172

33 px 7.74092

c

c Box For Inside Void

100 rpp -45 45 -15 15 -5 30

mode p e

c

c Materials

m4 12000. -0.01 \$ Aluminum (6061-T6)

13000. -0.9715 14000. -0.005 22000. -0.001

24000. -0.002 25000. -0.001 26000. -0.005

29000. -0.0025 30000. -0.002

m5 11000. -0.15307 \$ NaI(Ti) p= 3.67

53000. -0.8457 81000. -0.00123

m6 14000. -1 \$ Padding


```
m7 6000.04p      2 $ Reflector
   9000.04p      4
c
c Data Card
imp:p 1 1 1 1 1 1 0
imp:e 1 1 1 1 1 1 0
f8:e 16
e8 0.0 1024i 1.5
sdef par=2 pos=18 0 11.6 erg=D1
si1 L 0.00447 0.0318171 0.0321936 0.0364 0.66166
sp1 D 0.01 0.0196 0.036 0.0132 0.851
nps 2000000000
```